HAL open science

A biomimetic model of 3D fluid extracellular macromolecular crowding microenvironment fine-tunes ovarian cancer cells dissemination phenotype

Rümeyza Bascetin, Carine Laurent-Issartel, Cécile Blanc-Fournier, Charlotte Vendrely, Sabrina Kellouche, Franck Carreiras, Olivier Gallet, Johanne Leroy-Dudal

To cite this version:

Rümeyza Bascetin, Carine Laurent-Issartel, Cécile Blanc-Fournier, Charlotte Vendrely, Sabrina Kellouche, et al.. A biomimetic model of 3D fluid extracellular macromolecular crowding microenvironment fine-tunes ovarian cancer cells dissemination phenotype. Biomaterials, 2021, 269, pp.120610. 10.1016/j.biomaterials.2020.120610 . hal-03346495

HAL Id: hal-03346495

https://hal.science/hal-03346495v1

Submitted on 2 Jan 2023

HAL is a multi-disciplinary open access archive for the deposit and dissemination of scientific research documents, whether they are published or not. The documents may come from teaching and research institutions in France or abroad, or from public or private research centers.

L'archive ouverte pluridisciplinaire **HAL**, est destinée au dépôt et à la diffusion de documents scientifiques de niveau recherche, publiés ou non, émanant des établissements d'enseignement et de recherche français ou étrangers, des laboratoires publics ou privés.

Distributed under a Creative Commons Attribution - NonCommercial 4.0 International License

Version of Record: https://www.sciencedirect.com/science/article/pii/S0142961220308565
Manuscript_72c9348ae8c6c2da66a3422d07e7a821

A biomimetic model of 3D fluid extracellular macromolecular crowding microenvironment fine-tunes ovarian cancer cells dissemination phenotype

Rümeyza Bascetin [a,b *], Carine Laurent-Issartel [a], Cécile Blanc-Fournier [c], Charlotte Vendrely [a], Sabrina Kellouche [a], Franck Carreiras [a], Olivier Gallet [a*#], Johanne Leroy-Dudal [a#]

[a] ERRMECe, Equipe de Recherche sur les Relations Matrice Extracellulaire-Cellules (EA1391), Institut des matériaux I-MAT (FD4122), CY Cergy paris University, MIR, 1 rue Descartes, 95000 Neuville sur Oise Cedex, France.
Fax : +33 1 34 25 66 94

[b] Current address:
RNA Molecular Biology, F.R.S./FNRS, Université Libre de Bruxelles, Charleroi-Gosselies, Belgium

[c] Biological Ressources Centre "OvaRessources", certified NF S 96-900, Normandie University, UNICAEN, INSERM U1086 ANTICIPE, UNICANCER, Biopathology Department, Cancer Centre F. Baclesse, Caen, France

* Lead corresponding author: rumeyza.bascetin@gmail.com
* Corresponding author: olivier.gallet@cuy.fr

[#] Johanne Leroy-Dudal and Olivier Gallet are co-last authors

© 2020 published by Elsevier. This manuscript is made available under the CC BY NC user license
https://creativecommons.org/licenses/by-nc/4.0/

Abstract

An early fundamental step in ovarian cancer progression is the dissemination of cancer cells through liquid environments, one of them being cancer ascites accumulated in the peritoneal cavity. These biological fluids are highly crowded with a high total macromolecule concentration. This biophysical property of fluids is widely used in tissue engineering for a few decades now, yet is largely underrated in cancer biomimetic models. To unravel the role of fluids extracellular macromolecular crowding (MMC), we exposed ovarian cancer cells (OCC) to high molecular weight inert polymer solutions. High macromolecular composition of extracellular liquid presented a differential effect: *i*) it impeded non-adherent OCC aggregation in suspension and, decreased their adhesion; *ii*) it promoted adherent OCC migration by decreasing extracellular matrix deposition. Besides, there seemed to be a direct link between the extracellular MMC and intracellular processes, especially the actin cytoskeleton organization and the nucleus morphology. In conclusion, extracellular fluid MMC orients OCC dissemination phenotype. Integrating MMC seems crucial to produce more relevant mimetic 3D *in vitro* fluid models to study ovarian dissemination but also to screen drugs.

Keywords

Macromolecular crowding, extracellular matrix, ovarian cancer, spheroid, dissemination, migration

Abbreviations

Dx, dextran;

ECM, extra cellular matrix;

FBS, fetal bovine serum;

Fc, ficoll;

FVO, fractional volume occupancy;

mAb, monoclonal antibody;

MMC, macromolecular crowding;

NSI, nuclear shape index;

OCC, ovarian cancer cell;

pAb, polyclonal antibody;

SDS, sodium dodecyl sulfate;

TBS, Tris buffer saline;

TRIS, 2-amino-2-hydroxyméthylpropane-1,3-diol.

Introduction

An important challenge in ovarian cancer biology is to reproduce more relevant in vitro microenvironments. Designing this kind of tissue-specific tridimensional biomimetic model would help to understand the fine-tuning of cancer progression but could also be used as a more relevant model for drug screening. Although ovarian cancer mechanisms have been extensively examined at the molecular level, most of the studies are often uncoupled from the biophysical properties of the microenvironment. This microenvironment, which constantly confines cells, plays an important role in cancer development and dissemination as a source of many complex regulating signals including biological, biochemical but also biophysical signals [1–5]. A disruption in these signals induces variation in cell responses like transdifferentiation [6]. Major changes happen at many steps in cancer progression: tissue stiffening in the primary tumor site, dissemination through liquids in vascular and lymphatic networks and, implantation to secondary metastatic sites [7,8]. In the case of ovarian cancer, a unique alteration which arises at early stages is the shedding of cells from the primary site into the peritoneal cavity filled with a pathologic fluid called ascites [9,10]. At this step, ovarian cancer cells (OCC) are vehiculated by ascites to one of the main implantation site: the peritoneum covered with mesothelial cells. Cells are thus continuously confined in tailored crowded microenvironments, while *in vitro*, culture media are very diluted and far lower concentrated solutions with constant molecular composition [11,12]. Indeed, one crucial feature of biological systems, often underappreciated, is their high density of macromolecules, like proteins – glycoproteins - glycosaminoglycan - nucleic acids, present in a restricted volume. Such media are termed “crowded” rather than “concentrated“ as no single species of macromolecules is necessarily present at high concentration [13]. Macromolecular crowding (MMC) is a very well-known phenomenon in cell interior but is also observed in the extracellular microenvironment. As the density in the cell interior (including the nucleus) is 50-400 mg/mL [14–16], in multicellular organisms, cells are surrounded by a crowded extracellular environment, either a complex architectural extracellular matrix (ECM) network or a liquid environment. Biological fluids like blood, a vehicle for cancer cell dissemination, contain around 80 mg/mL of macromolecules [17]. Even if the exact concentration is not described, the high density of macromolecules in ECM surrounding cells is well known [18]. Lastly, in the case of ovarian cancer, cells can also disseminate to metastatic sites through a peculiar liquid called ascites accumulated in the peritoneal cavity of unhealthy women and known for its high density of macromolecules [19,20]. The impact of ECM physical properties (like stiffness and porosity) and fluids dynamic (like shear stress) on cells have been extensively studied while the role of fluids MMC is still underappreciated [21–23]. In the case of ovarian cancer, ascites play an important role in ovarian cancer dissemination. Ascites are complex and heterogeneous fluids thus harboring specific chemical and physical properties. This suggests that they could create a confined and crowded microenvironment at the surface of the peritoneum affecting OCC implantation. For example, a fibrin network was shown to entrap OCC on mesothelial tissue [24]. It is thus substantial to understand the role of fluids MMC in ovarian cancer development to design relevant biomimetic liquid models for cancer model engineering and drug discovery.

“Macromolecular crowding” is defined by the non-specific influence of steric repulsions on specific processes occurring in highly volume occupied media. Therefore, molecular crowding has been shown to significantly

alter biological, biochemical, and biophysical properties by: *i)* inducing an excluded volume effect where the volume occupied by co-solute is inaccessible to other molecules, *ii)* affecting molecules folding, *iii)* slowing down diffusion and, *iv)* increasing the binding reaction of molecules [25–28]. Altogether, these properties of MMC lead to crucial impacts on cellular properties including intracellular as well as extracellular events.

In the nucleus, intracellular crowding plays a role in micro-compartmentalization of chromatin [29,30]. Thus, intracellular crowding is involved in gene expression as it : *i)* slows down the diffusion of molecules like transcription factor, *ii)* increases association rate of DNA-binding proteins like RNA polymerase and, *iii)* decreases dissociation [28,31,32]. In the cytoplasm, intracellular crowding affects transcription factors nuclear translocation, intracellular signalization, vesicle trafficking and cytoskeleton [33–36]. Several studies showed that intracellular crowding is a fundamental constraint for cell metabolism as it limits free space inside cells and so the maximum enzyme and mitochondria concentration. This crowding imposes the activation of different energy generation pathways, called the Warburg effect, to provide enough ATP supply to highly proliferative and/or active cells [37]. Intracellular crowding induced by hypotonic stress can provoke endogenous irreversible protein aggregation [38]. Intracellular overcrowding due to protein aggregation can induce a progressive switch of energy generation pathway but also decrease the maximum energy generation capacity [39]. These suppose that beyond a concentration of protein aggregates, cells cannot even satisfy their basal energy demand and eventually lead to “metabolic cell death by overcrowding”. This process could possibly be implicated in neuropathological diseases [39]. *In vitro*, molecular crowding has been shown to regulate protein structure by promoting their aggregation and/or amyloid formation [40–45].

In the extracellular space, molecular crowding enhances enzymatic reaction at cell surfaces, and promotes autocrine signaling by limiting diffusion of molecules from their production source to increase their concentration locally [25,46]. Thus, extracellular MMC enhances ECM deposition by human fibroblast and by human bone marrow mesenchymal stem cells [12,47–53]. While almost no information is available about other ECM protein apart their enhanced deposition, the mechanism of collagen deposition has been more extensively studied under MMC. Lareu *& al.* showed that enhanced collagen matrix deposition by normal primary embryonic lung fibroblasts was due to an increase in Procollagen C proteinase enhancer protein helping Procollagen C-proteinase to convert pro-collagen in collagen [48]. Several studies showed the stabilization of collagen ECM correlated with an increase of lysyl oxidase and transglutaminase activity in crowded environments [47,54,55]. Moreover, MMC shortens the lag phase of collagen fibrillogenesis thus, collagen fibrils are formed more rapidly but thinner [56,57]. Another study proposes that crowders, especially dextran sulfate, can drive ECM deposition by increasing electrostatic protein aggregation independently from their crowding capacities [58]. Zeiger & al also revealed that MMC induces supramolecular assembly and alignment of extracellular collagen IV and fibronectin, which in turn also increase intracellular actin cytoskeleton alignment [12].

In the extracellular microenvironment, MMC can also help to maintain the undifferentiated state of stem cells in their niche or either promote their differentiation outside the niche [46,49,52,53,59]. This property of MMC

to improve ECM deposition and cell culture is of principal interest for tissue engineering to maintain specialized cells like podocytes and accelerate *in vitro* patient autologous tissue production which is usually too long (196 days for blood vessels) [53,60,61].

So far, and as described above, many works provided information on the effect of intracellular MMC on gene expression, metabolism, and protein assembly. Many works showed the beneficial effect of extracellular MMC on matrix deposition and healthy cell behaviors. But only a few studies have been carried out to understand the effect of extracellular MMC on unhealthy cells in pathological conditions. Vazquez *et al*. discussed the relationship between intracellular crowding and metabolism in cancer cells and neuropathological diseases [37,39]. Two works used extracellular MMC to mimic fibrotic-like matrix and screen anti-fibrotic agents [47,62]. Gonzalez *et al*. showed the differential responses of normal versus liver cancer cells, and cancer derived-endothelial cells in crowded environments [63,64]. Sun *& al.* used crowding to fractionate and isolate nuclear protein in normal and cancer cells [36]. And lastly, Ranamukhaarachchi *& al.* used crowding to tune collagen gel architecture and studied breast cancer cells morphology and invasiveness [65]. Ovarian cancer is one of a kind to be directly in contact with the biological crowded fluids ascites. But, no studies on the effect of extracellular fluids MMC neither decellularized matrix produced in crowded environment seems to be reported on ovarian cancer.

Our work provides appreciable insights as studies are scarce in the literature regarding the direct relationship between fluid extracellular MMC and ovarian cancer development and behavior, a peculiar cancer disseminating from early stages through the liquid called ascites. Our data pointed at the differential role of extracellular MMC on adherent and non-adherent OCC: extracellular MMC impaired adhesion and aggregation of non-adherent OCC; extracellular MMC increased adherent OCC migration through alteration of ECM deposition. Extracellular MMC also potentially regulates intracellular processes like cytoskeleton organization and gene expression in the nucleus. The more the crowder is crowding, the more the impact on OCC would be important with a higher impact on mesenchymal-like OCC. The present work has been done to decipher the role of fluid extracellular MMC on OCC behaviors and matrix deposition with the future purpose of generating more relevant 3D *in vitro* liquid models for ovarian cancer study, drug screening, and tissue-specific tailoring.

Materials & Methods

Antibodies and reagents

Dapi (4,6-diamidino-2-phenylindole dihydrochloride, D9542) and fluorescein isothiocyanate-labeled phalloidin (p5282) were purchased from Sigma-Aldrich (France). Prolong® Gold Antifade Reagent (P36930) was supplied by ThermoFisher Scientific (France).

Ficoll 400 kDa was purchased from Ge Healthcare (17-0300-10). Dextran 200 (average molecular weight 250 kDa) was from Serva (SERA18694).

Polyclonal (pAb) and monoclonal (mAb) antibodies used in this study and their dilution for immunofluorescence and western blot assay are reported in Table S1 (Supplemental material).

Cell culture

Human adenocarcinoma cell line IGROV1 was kindly provided by Dr. J. Bénard from the INSERM U1199 BioTICLA unit (Biologie et Thérapies Innovantes des Cancers Localement Aggressifs, Caen, France) and SKOV3 cells were purchased from ATCC (France) with a certificate of conformity. Cells were cultured in a humidified atmosphere at 37°C and 5% CO_2 in their complete medium consisting of RPMI-1640 GlutaMAX (Life technologies, France) supplemented with 10% fetal bovine serum (FBS, Biosera, France) and 1% sodium bicarbonate (Invitrogen, Cergy, France). For experiments, cells were cultured in their complete medium supplemented with different concentrations of Ficoll or Dextran.

Cell proliferation assay

Cells were harvested with trypsin-EDTA 0.25%, seeded in 48-well plate at 10^4 cells/cm^2, and incubated 24h in their complete culture medium. Adherent cell proliferation was then monitored over seven days in their complete culture medium supplemented with 0 or 75 mg/mL of Ficoll or Dextran. At each time point, representative images were captured by phase-contrast microscopy with the objective 10x. At each time point, cells were harvested with trypsin-EDTA 0.25% and counted with Trypan Blue (T8154, Sigma, France). Results are represented as the mean of cell number ± standard deviation of at least three independent experiments in duplicate.

Cell metabolic activity

Cells were harvested with trypsin-EDTA 0.25%, seeded in 96-well plate at 15.10^3 cells/cm^2, and incubated 24h in their complete culture medium. Adherent cell metabolic activity was then monitored over seven days in their complete culture medium supplemented with 0 or 75 mg/mL of Ficoll or Dextran. At each time point, the culture medium was replaced by XTT reagents (Cell proliferation Kit II, Roche, France) and cells were incubated for 2h at 37°C. Cell metabolic activity was estimated by absorbance measurement at 475 nm. Results are represented as the mean of absorbance of triplicate.

Spheroid formation assay

Cells were harvested with trypsin-EDTA 0.25% and suspended at 10^4 cells/10 µl of complete culture medium supplemented with 0 or 75 mg/mL of Ficoll or Dextran. Pending droplets of 10 µl were formed on the inward face of 24-well plate and cultured for 24h at 37°C. Cell aggregates were observed and captured by phase-contrast microscopy with the objective 4x.

Cell adhesion assay

Cells were harvested with trypsin-EDTA 0,25%, seeded in a 96-well plate at 5.10^4 cells per well in complete culture medium supplemented with 0, 12.5, 25, or 75 mg/mL of Ficoll or Dextran, and incubated 30 minutes at 37 °C and 5% CO_2. Non-adherent cells were then washed three times with serum-free medium. Remaining adherent cells were fixed with glutaraldehyde (1% in distilled water) (G4004, Sigma-Aldrich, France) for ten minutes. Wells were washed three times with distilled water and counted on three fields with the objective 10x. Results are represented as the mean of cell percentage ± standard deviation of two independent experiments in triplicate. Data are expressed as a percentage of the control condition without crowders.

Cytoplasmic actin and vinculin analysis

SKOV3 and IGROV1 cells were seeded on glass coverslips at 5.10^3 cells/cm^2 in 48-well plate for 6h. Cells were then starved overnight in serum-free medium and cultured for 6h in complete medium supplemented with 0 or 75 mg/mL of Ficoll or Dextran. Actin and vinculin were immunostained, and cells were imaged by confocal microscopy with the objective 63x (LSM710, Zeiss, Germany). Results are representative of at least two independent experiments in duplicate.

Cell migration assay

SKOV3 and IGROV1 cells were grown as a monolayer for 24h in their complete culture medium using ibidi© culture-insert 2 well (BioValley, France) with respectively 15.10^3 and 40.10^3 cells/insert well. Culture inserts were then removed. Cells were rinsed with serum-free medium and incubated in their complete culture medium supplemented with 0 or 75 mg/mL of Ficoll or Dextran, at 37°C and 5% CO_2. Cell migration was monitored with the objective 10x by inverted time-lapse microscopy (DMI6000B, Leica, Germany) for 4h at regular time intervals of 15 minutes.

Extracellular matrix analysis

SKOV3 and IGROV1 cells were seeded respectively at 4.10^4 and 7.10^4 cells/cm^2 for 24h. Adherent cells were then incubated for 48h in their complete culture medium supplemented with 0 or 75 mg/mL of Ficoll or Dextran. Fibronectin, vitronectin, collagen I, collagen IV, and laminin were detected by immunofluorescent staining. Cells were imaged by confocal microscopy with the objective 63x (LSM710, Zeiss, Germany). Results are representative of two independent experiments in duplicate.

Immunofluorescent staining

Cells were fixed with 3% paraformaldehyde for 10 minutes and permeabilized with PBS-Triton X-100 0.1% for 3 minutes. For cytoskeleton visualization, cells were stained for actin with FITC-phalloidin (10 µg/mL) and nuclei with DAPI (0.3 µg/mL) in PBS-BSA 1% for 30 min. For other proteins staining, non-specific sites were blocked 30 minutes with PBS-BSA 1% and incubated overnight at +4°C with primary antibodies (in PBS-BSA 1%). After three washes with PBS, cells were incubated 1h at room temperature in the dark with their respective Alexa fluor-conjugated antibody (in PBS-BSA 1%) and stained 30 minutes at room temperature in the dark with DAPI at 0.3 µg/mL (in PBS-BSA 1%). Coverslips were mounted with Prolong® Gold Antifade Reagent and imaged by confocal microscopy with the objective 63x (LSM710, Zeiss, Germany). Controls, where primary antibodies were replaced with PBS-BSA 1%, were negative.

Nuclear area and nuclear shape index

From the different fluorescence images acquired on SKOV3 and IGROV1 cells cultured for 48h in culture media supplemented with 0 or 75 mg/mL of Ficoll or Dextran, nucleus area and nucleus shape index were determined with the Particle Analysis tool of ImageJ® software (National Institutes of Health, Bethesda, MD). The nuclear shape index (NSI) represents how much the nucleus is circular or linear [4]. NSI is comprised between 0 and 1. An NSI value tending toward 1 represents a circular object while a value of 0 matches with an elongated object. At least 827 SKOV3 and 1512 IGROV1 cells (SKOV3: min 827 - max 1827; IGROV1: min 1512 - max 2242) for each treatment group (0 or 75 mg/mL of Ficoll or Dextran) were analyzed per experiment from at least four independent experiments in duplicate.

Western blotting of conditioned cell growth media proteins

SKOV3 and IGROV1 cells were seeded respectively at 4.10^4 and 7.10^4 cells/cm^2 for 24h. Adherent cells were then incubated for 48h in their complete culture medium supplemented with 0 or 75 mg/mL of Ficoll or Dextran. Supernatants were then recovered and their total protein concentration was assessed with the Bicinchoninic Acid Protein Assay kit (BCA1 and B9643, Sigma, France) according to the manufacturer's instruction and with Bovine Serum Albumin (P0914, Sigma, France) as standard. 100 µg of supernatant proteins were subjected to 8% bis-acrylamide SDS-PAGE electrophoresis under denaturing and reducing conditions and transferred onto a reinforced nitrocellulose membrane (GE Healthcare, Life Sciences, France) for 1h at 110V and +4°C. The membrane was blocked for 1h at room temperature with TTBS (50 mM Tris–HCl, 150 mM NaCl pH 7.4, 0.1% Tween 20) supplemented with 5% (w/v) defatted dry milk. The membrane was incubated overnight at +4°C in TTBS-milk 3% with the primary antibody. After three washes with TTBS, the membrane was incubated for 1h at room temperature in TTBS-milk 3% with the horseradish peroxidase-conjugated antibody. After three washes with TTBS, the immunoreactivity was detected by enhanced chemiluminescence (WBKLS0500, Millipore) according to the manufacturer's instruction. Proteins were revealed using ImageQuant LAS 500 (GE Healthcare Life Sciences, France).

Statistics

Data are expressed as mean ± standard deviation. Statistical significances were determined by the appropriate test as indicated in figure captions.

Significance levels were set compared to the control without crowders: $p < 0.05$ (*), $p < 0.01$ (**), $p < 0.005$ (***).

Results

Extracellular MMC differentially affects OCC proliferation

Ovarian cancer cells (OCC) disseminate through liquids: primarily ascites accumulated in the peritoneal cavity of unhealthy women and, other body fluids. We estimated a total protein concentration of around 75 mg/mL in two human blood plasma and three human ovarian cancer ascites (Figure S1) [17,20]. We also previously showed that both ascites and blood plasma contains high molecular weight molecules and especially fibronectin (200-250kDa as a monomer and 400-500 kDa as a dimer) which has a preponderant role in regulating cell responses [4,66,67]. To mimic the macromolecular crowding derived from the presence of high molecular weight molecules in these two biological fluids, cells were exposed to two commonly used inert crowders: Ficoll 400 kDa (Fc) or Dextran 250 kDa (Dx) at the concentration of 75 mg/mL, representing the total protein concentration estimated in blood plasma and ovarian cancer ascites. Fc is a deformable spherical molecule composed of a highly branched copolymer of sucrose and epichlorohydrin, while Dx is a flexible ribbon-like molecule. Each of them could respectively mimic the globular and fibrillar/unfolded state of biological molecules like fibronectin. Per literature, we showed that these two crowders have few similar biophysical features: a hydrodynamic radius (Rh) of around 5 nm, a polydispersity index of around 0.46 and, a neutral net charge. However, these two crowders also present different features: their molecular weight and thus their different fractional volume occupancy (FVO) of 6.6% and 10% respectively for Fc and Dx (Figure S2) [48,52,55,68–72]. In this study, we especially chose these two inert crowders as we wanted to mimic and analyze solely the effect of MMC. We could thus evaluate the effect of MMC derived from two different high molecular weight inert molecules without the interference of charge and Rh but still yielding for different FVO/crowdedness. This could help in understanding if these two crowders have either the same effect on OCC and determine the sole effect of crowding/FVO.

In this study, we worked with two OCC: SKOV3 cells with an intermediate-mesenchymal phenotype isolated from ascites and IGROV1 cells with an intermediate-epithelial phenotype originating from a primary tumor site [3,73,74]. The proliferation of SKOV3 and IGROV1 cells estimated by counting cells with trypan blue, and their metabolic activity checked with an XTT assay was assessed in medium supplemented with 0 or 75 mg/mL of Fc or Dx (Figure 1). With Fc, both cell numbers increased and reached a plateau similarly to the control without MMC over seven days (Figure 1B). With Dx, a stagnating SKOV3 cell number was observed upon the seven days of culture and IGROV1 cell number was three times less important compared to the control. These results were strengthened by phase-contrast microscopy: SKOV3 and IGROV1 cells covered the culture surface without MMC and with Fc within the seven days of culture - in the presence of Dx, SKOV3 cells did not proliferate but changed their morphology to form small cell aggregates; IGROV1 cells proliferation was greatly slowed down (Figure 1D).

Correlating with the proliferation, the metabolic activity of both cell types increased within the seven days of culture and reached a plateau without MMC or with Fc (Figure 1C). The metabolic activity of SKOV3 cells cultured with Dx remained stagnant similarly to the proliferation curve, indicating that cells did not die. Surprisingly, while IGROV1 cell proliferation with Dx was highly decreased of about 72% compared to the control, metabolic activity was only decreased by 38%. This suggests that Dx-associated MMC still enhances

IGROV1 cell metabolic activity. To determine if MMC induced senescence of OCC, we performed a senescence-associated β-galactosidase activity assay. As observed in Figure S3, no significant β-galactosidase-associated blue staining was detected in both cell types.

Carduner *& al*. showed that OCC culture in ovarian cancer ascites induced their detachment from substratum to form multicellular aggregates in suspension [3]. Here, contrary to ascites, over the seven days of culture, we did not notice any cell detachment with neither Fc nor Dx (Figure 1D).

Altogether, these data indicate that the two mimetic crowded environments have different effects on OCC proliferation: Fc does not impair cell proliferation and metabolic activity while more crowding Dx has a cytostatic effect and attenuates cell proliferation with a more prominent effect on mesenchymal SKOV3 cells. Still, Dx seems to increase the metabolic activity of IGROV1 cells.

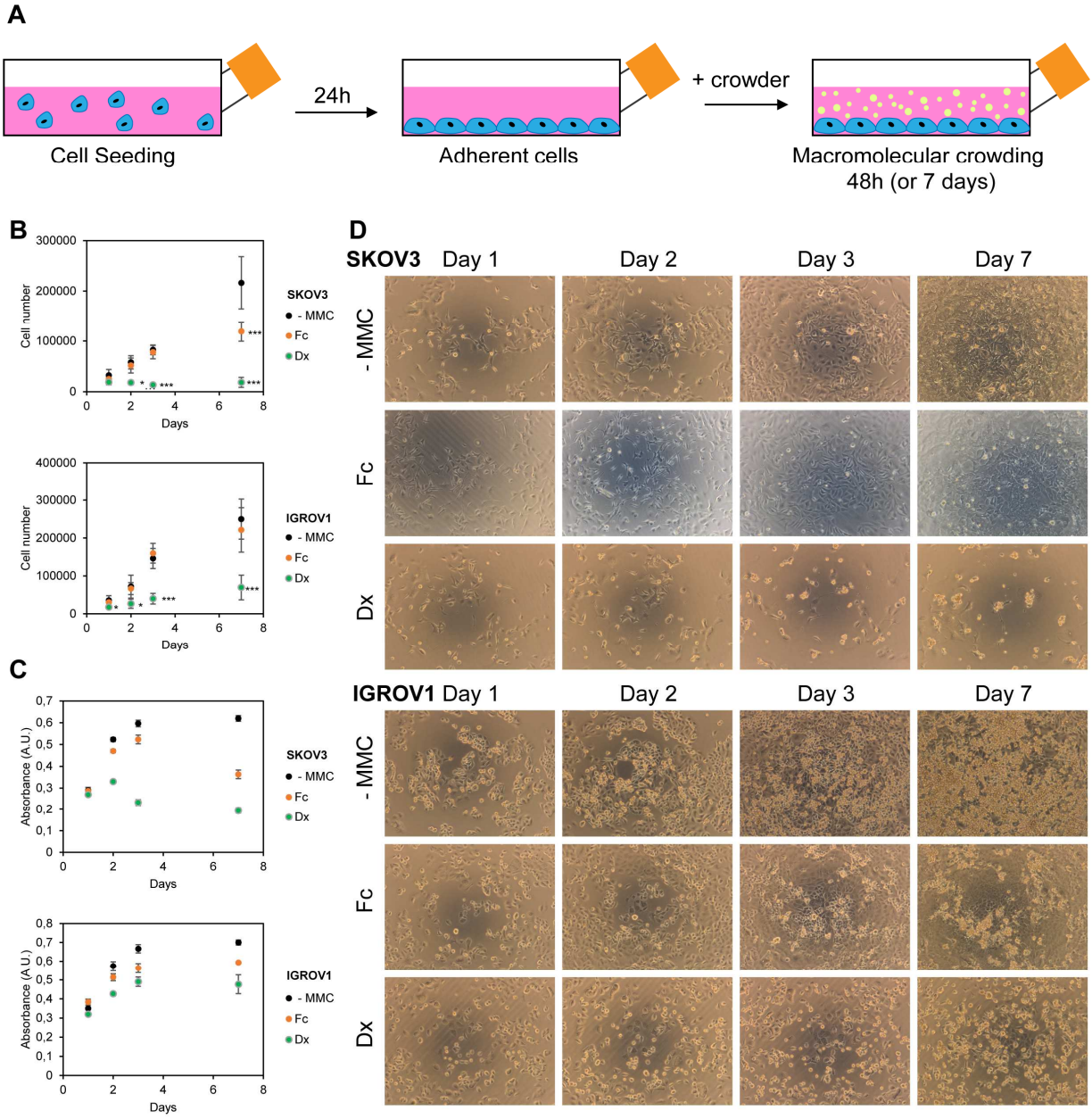

Figure 1. Extracellular macromolecular crowding affects OCC proliferation and metabolic activity. (A) Except for adhesion and spheroid assay, SKOV3 and IGROV1 cells adhered for 24h in their culture media before changing their media to fresh culture media supplemented with 0 (-MMC) or 75 mg/mL of Fc or Dx. Cells were then cultured for 48h (or seven days for proliferation and metabolic activity assay). (B) Cell counting with Trypan blue monitored over seven days of culture, revealed Fc does not affect cell proliferation, while Dx slows down it. Results are represented as the mean of cell number ± standard deviation of two independent experiments in triplicate. Significant differences were estimated by comparison with control without crowders (-MMC) (*** $p < 0.005$, Student's test). (C) XTT assay shows that Fc does not affect cell metabolic activity while Dx differentially affects SKOV3 and IGROV1 metabolic activity. (D) Representative images of cells over the proliferation time course are presented for SKOV3 and IGROV1 cells cultured with 0 (-MMC) or 75 mg/mL of Fc or Dx. Scale bar: 100 µm.

Extracellular MMC prevents OCC spheroid formation

Upon their detachment, ascites promotes the compaction of OCC in multicellular aggregates named spheroid compared to culture media (Figure S4) [75]. Thus, we looked at the spheroid formation by non-adherent SKOV3 and IGROV1 cells using the pending droplet method (Figure 2). Without MMC, we observed that both cell types gathered together to form a “single multicellular aggregate”. Both cell types spheroid was altered in a concentration-dependent manner with the increasing concentration of Fc and Dx. The effect was more pronounced with SKOV3 cells which were single isolated at 75 mg/mL of Dx, while IGROV1 cells formed small aggregates. Thus, extracellular MMC prevents the aggregation of non-adherent OCC into large spheroid in a liquid environment.

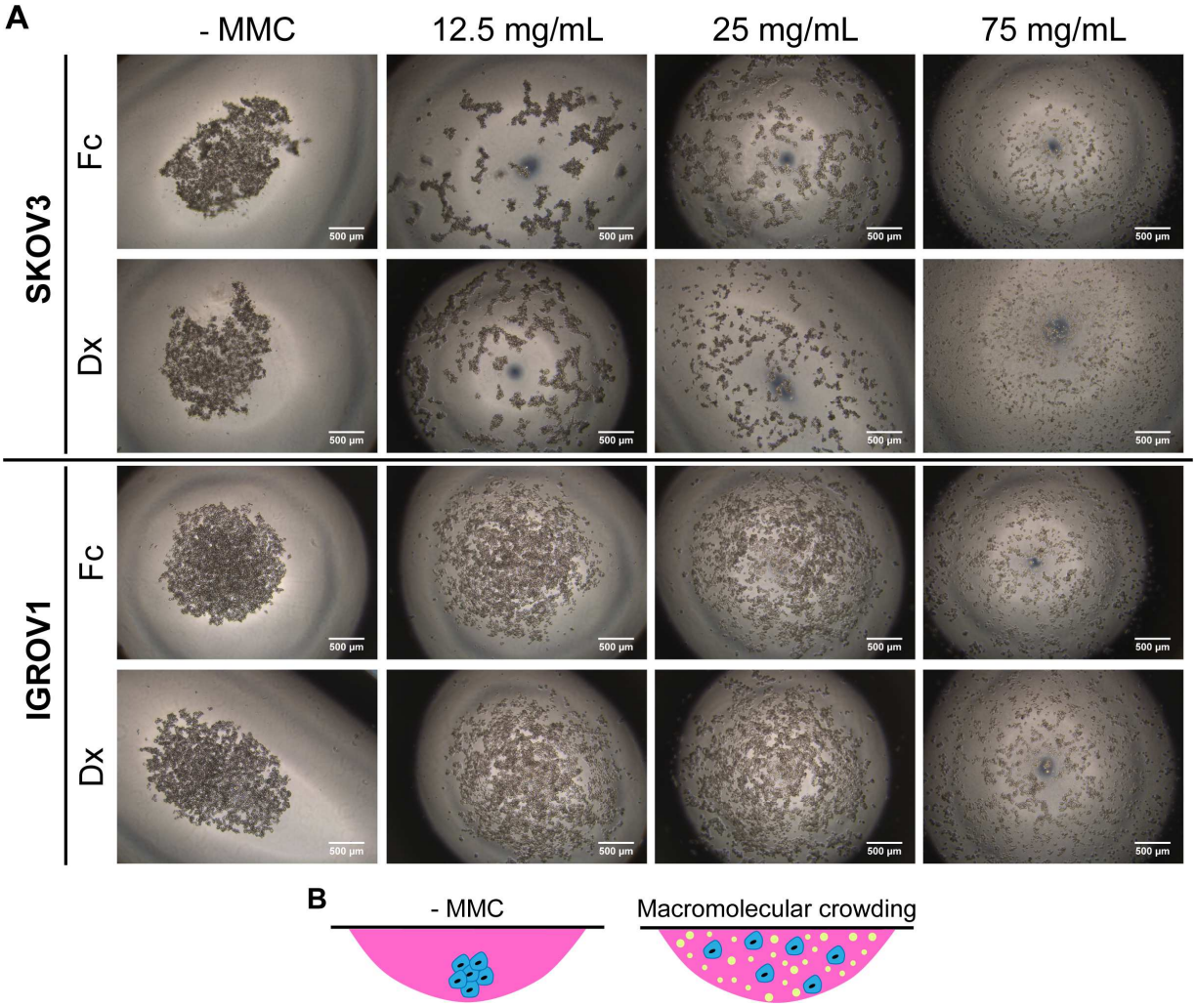

Figure 2. Extracellular macromolecular crowding impedes OCC spheroid aggregation. (A) Spheroids were formed by 10^4 non-adherent SKOV3 (upper panel) or IGROV1 (lower panel) cells in culture medium droplet supplemented with either 0 (-MMC), 12.5, 25, or 75 mg/mL of Fc or Dx for 24h. Representative images show that Fc and Dx prevent large spheroid formation. Scale bar: 500µm. (B) Schematic representation of cell aggregation in culture media or crowded media.

Extracellular MMC prevents OCC adhesion

One of the main events in cancer development is the implantation of OCC on distant organs to further disseminate. That is why we looked at the effect of extracellular MMC on OCC adhesion and spreading onto culture substratum (Figure 3). Compared to the control without MMC, cell adhesion increased by about 40 and 24.6 % respectively for SKOV3 and IGROV1 cells in the presence of 12.5 mg/mL of Fc (Figure 3A). Although cell adhesion percentage was similar to the control in the presence of 25 mg/mL of Fc, cell adhesion significantly decreased to 30.2 and 52.4 % respectively for SKOV3 and IGROV1 cells in the presence of 75 mg/mL of Fc. The decline in cell adhesion was even more drastic with Dx. Cell adhesion significantly dropped to 20.4, 7.6, and 4.8% in the presence of respectively 12.5, 25 and 75 mg/mL of Dx in the case of SKOV3 and decreased to 62.2, 56.5 and 10% in the case of IGROV1 cells. The impact of Dx is once again more prominent on mesenchymal-like

SKOV3 cells than on epithelial-like IGROV1 cells. Here, we show that high MMC prevents OCC adhesion to the substratum and even more if MMC has a higher FVO like in the case of Dx.

We further looked at the effect of extracellular MMC on adherent OCC actin organization immunostained upon their culture in the presence of 0 or 75 mg/mL of Fc or Dx (Figure 3B). Without MMC, SKOV3 and IGROV1 cells were well spread, presented peripheral cortical actin and/or central stress fibers. With Fc, both cell types still presented cortical actin and stress fiber but to a lesser extent. With Dx, SKOV3 and IGROV1 cells spreading area was significantly reduced. They seemed to organize diffuse perinuclear actin caps.

We then visualized the anchoring structures of OCC by immunostaining vinculin (Figure 3C). Dash-like structures, corresponding to focal adhesions, at the peripheral of SKOV3 cells were observed without MMC (Figure 3C). With Fc, SKOV3 cells presented fewer focal adhesions while with Dx only large peripheral dot-like anchoring sites were seen. IGROV1 cells presented central fibrillar adhesions in control condition witnessing strong cell adhesiveness (Figure 3C). With Fc, focal adhesions at the peripheral of IGROV1 cells were observed with only a few fibrillar adhesions. With Dx, only large peripheral anchoring sites were observed. These results hint at the less mature organization of anchoring sites when cultured in crowded environments and could also explain the decrease in OCC adhesion.

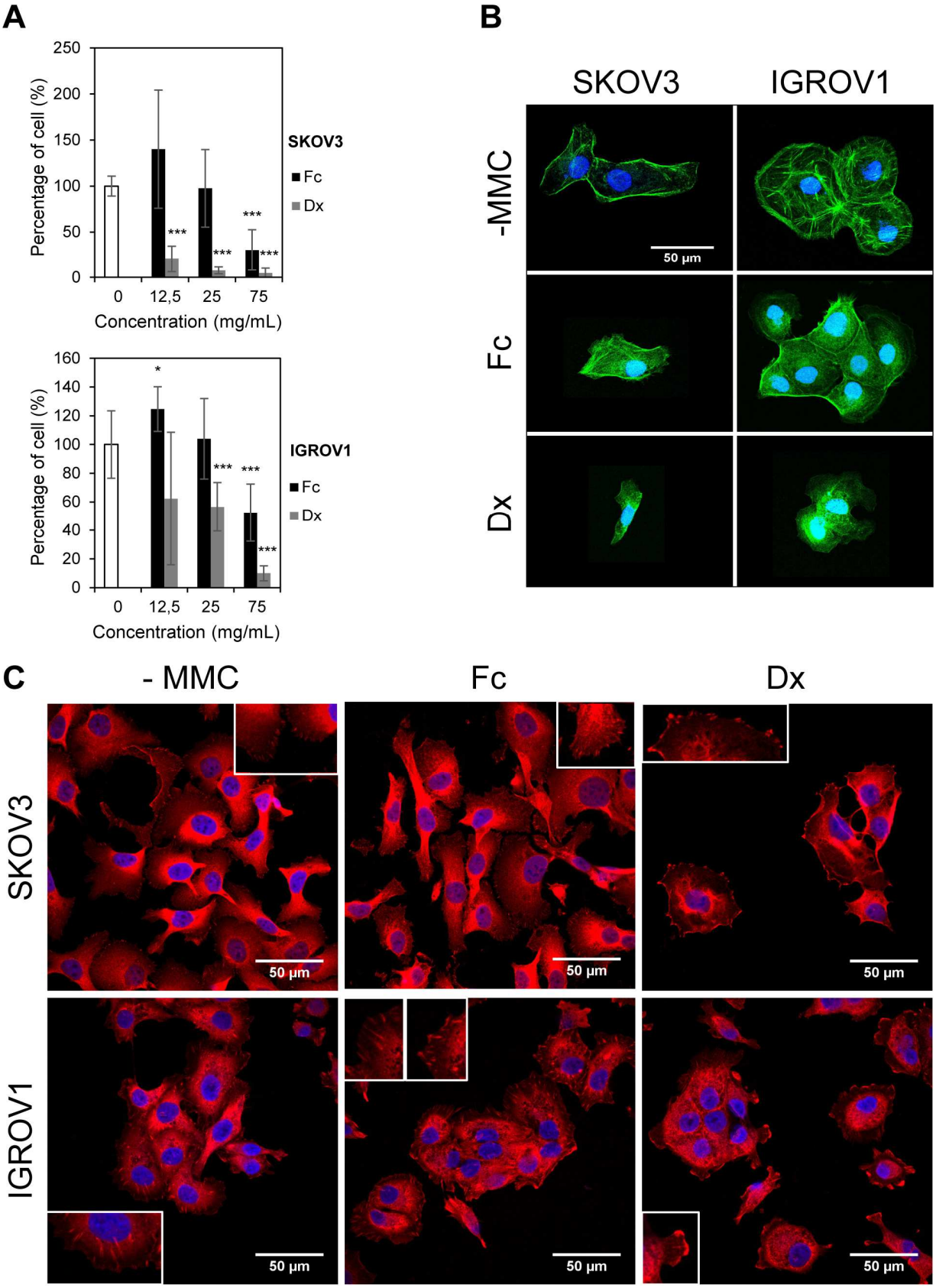

Figure 3. Extracellular macromolecular crowding alters OCC adhesion. (A) Adherent SKOV3 and IGROV1 cells were counted after 30 minutes of seeding in their culture media supplemented with either 0, 12.5, 25 or 75 mg/mL of Fc or Dx. Results show that high MMC decreases cell adhesion. Results are represented as the mean of the percentage of adherent cell ± standard deviation of two independent experiments in triplicate. Significant differences were estimated by comparison with control without crowders (* $p < 0.05$; *** $p < 0.005$,

Student's test). (B) Adherent SKOV3 and IGROV1 cells were starved overnight in serum-free medium, and cultured 6h in their culture media supplemented with 0 (-MMC) or 75 mg/mL of Fc or Dx. Cells were then stained for actin (green) and DNA (blue), or vinculin (red) and DNA (blue). Representative images, of two independent experiments in duplicate, reveal the reorganization of the actin cytoskeleton and anchoring sites in crowded environments. Scale bar: 50 µm.

Extracellular MMC differentially promotes OCC migration

As the different results point at a potential effect of extracellular MMC on adherent OCC motility, scratched cell monolayer was monitored in the presence of 0 or 75 mg/mL of Fc or Dx (Figure 4). Without MMC, SKOV3 cells migrated collectively (blue arc). With Fc, SKOV3 cells covered a more important surface, seemed to preserve a collective migration but also presented individual migration patterns (white arrow) as observed with cells scattered in the open wound area. With Dx, even if the migration rate was not as important as with Fc, SKOV3 cells also migrated but in a more scattered manner. IGROV1 cells almost did not migrate without MMC but still presented a few collective migration fronts. With Fc, cells covered a higher distance collectively (blue arc) and with few cells scattering in the open wound area (white arrow). With Dx, IGROV1 also did not migrate as much as with Fc, but they seemed to migrate in a collective as well as individual manner. These results hint at the differential effect of MMC on cell migration: Fc accelerates collective and individual migration of OCC; more crowding Dx promotes a more scattered migration with a lesser impact on cell velocity.

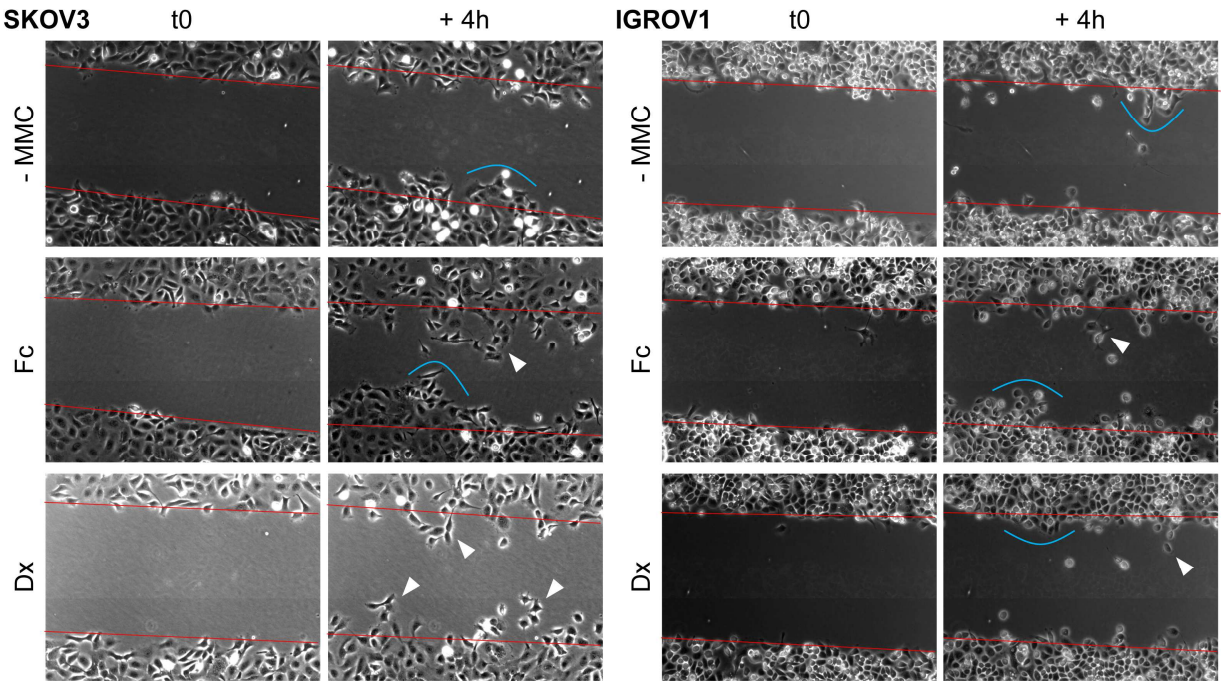

Figure 4. Extracellular macromolecular crowding affects OCC migration. SKOV3 and IGROV1 cell migration was monitored for 4h in their culture media supplemented with 0 (-MMC) or 75 mg/mL of Fc or Dx. Blue arcs point at the collective migration front and, white arrows point at the scattered individually migrating cells. Representative images reveal a differential effect of Fc and Dx on SKOV3 and IGROV1 cells.

Extracellular MMC differentially affects tight and adherent junction protein

To further investigate the effect of MMC on adherent OCC, we looked at the intercellular junction in the presence of 0 or 75 mg/mL of Fc or Dx. We immunostained two junction proteins: tight junction scaffolding protein ZO-1 and transmembrane adherent junction protein E-cadherin (Figure 5) [76]. Without MMC, SKOV3 cells presented a faint linear pattern of ZO-1 at cell-cell junctions. Surprisingly, with Fc or Dx, a more intense and jagged ZO-1 organization was observed. Junctional E-cadherin could not be detected in SKOV3 cells monolayer. Nevertheless, a more pronounced nuclear E-cadherin staining in SKOV3 cells could be observed when cultured with Dx and to a lesser extent with Fc. IGROV1 cells presented well defined intense, linear, and continuous ZO-1 junctions with no modification whatever the culture condition. Well defined intense, linear, and continuous E-cadherin junctions could also be observed without MMC or with Fc at the periphery of IGROV1 cells. With Dx, there seem to be fewer E-cadherin junctions. Here, we show a direct link between extracellular MMC and intercellular junction proteins organization with a differential effect depending on cancer cells phenotype: increase of ZO-1 junctions and potentially nuclear E-cadherin in case of mesenchymal-like SKOV3 cells and a decrease in E-cadherin junctions in epithelial-like IGROV1 cells.

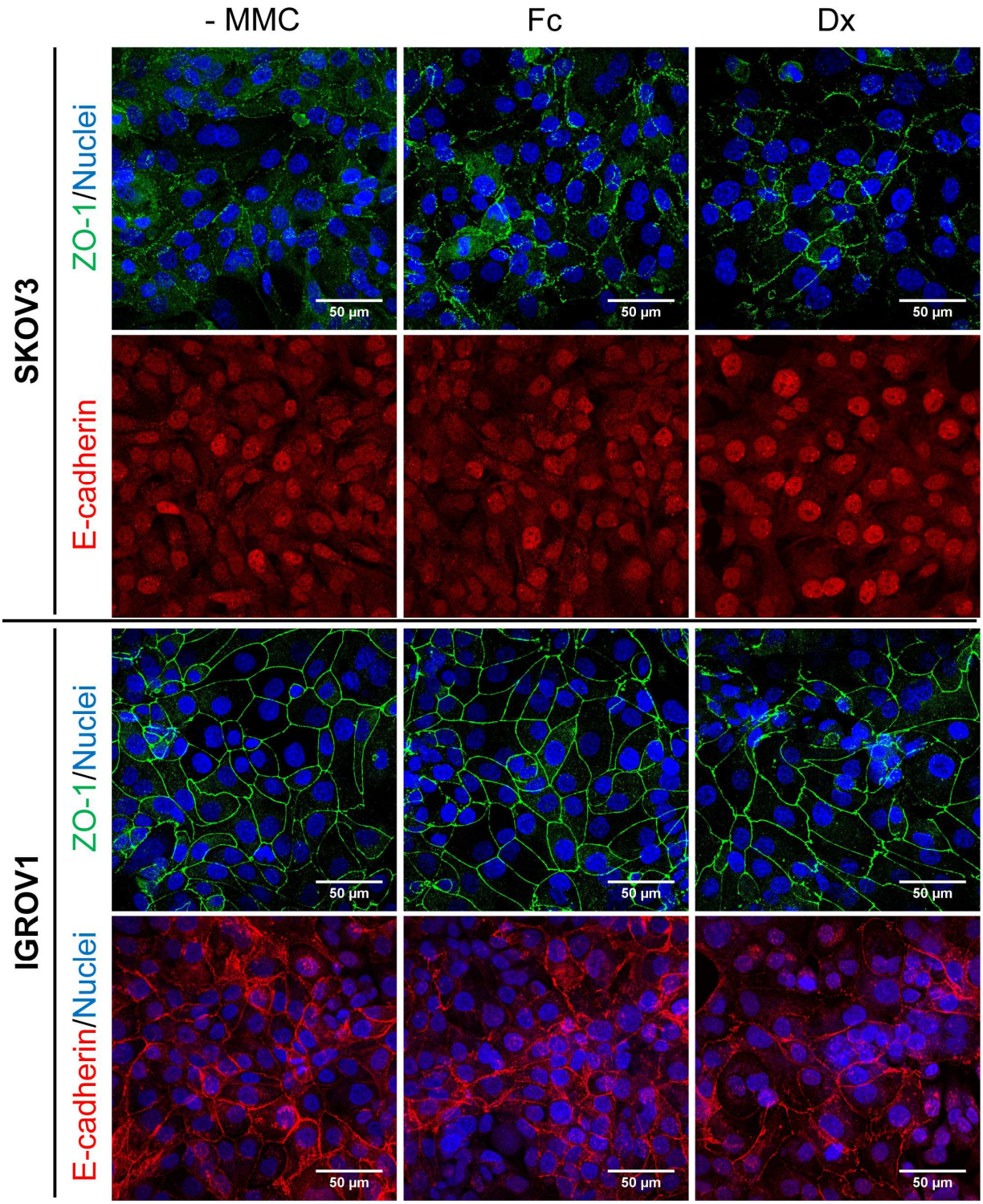

Figure 5. Extracellular macromolecular crowding modulates OCC intercellular junction proteins organization. Adherent SKOV3 and IGROV1 cells were cultured 48h in their culture media supplemented with 0 (-MMC) or 75 mg/mL of Fc or Dx. They were then stained for ZO-1 (green) or E-cadherin (red) and DNA (blue). Representative images show the differential effect of MMC on cells, with an increased intercellular ZO-1 and nuclear E-cadherin in SKOV3 cells and a decreased intercellular E-cadherin in IGROV1 cells. Scale bar: 50 µm.

Extracellular MMC differentially affects OCC extracellular matrix

We immunostained stromal ECM proteins - fibronectin (Fn), vitronectin (Vn), collagen I (CollI) - and basal membrane proteins – laminin (Lam), collagen IV (CollIV) - deposited by SKOV3 and IGROV1 cells cultured in the presence of 0 or 75 mg/mL of Fc or Dx (Figure 6A). Similarly to the control without MMC, with of Fc, SKOV3 cells organized an intense Fn matrix with some fibrils, only a few spots of Vn and CollI, a diffuse but dense Lam matrix, and a faint CollIV matrix (Figure 6A). With Dx, no differences were seen in Vn, CollI, and CollIV deposition. Still, a decrease in Fn and Lam deposition was observed. IGROV1 cells deposited less matrix, but a similar pattern as SKOV3 cells was observed with and without MMC. We performed similar immunostaining to analyze the ECM network of normal mesothelial Met5A cells (covering the peritoneal cavity of women) in crowded complete or serum-free media. The results revealed a similar pattern to OCC. With Fc, the deposition of Fn, CollI, Lam and CollIV was a little decreased compared to the control without MMC, while their deposition was considerably decreased with Dx (Figure S5). Contrary to previously published works, MMC has the opposite effect on matrix deposition than that observed on healthy fibroblast or stem cells in literature. Here, extracellular MMC induces a decrease in ECM deposition by unhealthy OCC and normal mesothelial cells.

The conditioned growth media of OCC with Fc or Dx has been harvested and submitted to western blot. Compared to the control, the supernatant of SKOV3 cells cultured with Fc revealed a drastic decrease of Lam and a slight decrease of Fn, CollI 45 kDa fragment, and Vn 65 kDa isoform (Figure 6B). An increase of Vn 40 kDa and smaller fragments was observed. With Dx, these observations were even more pronounced. The supernatant of IGROV1 cells cultured with Fc also presented a decrease in Lam, Fn, and CollI 45 kDa fragment and, Vn 40 kDa and smaller fragments. With Dx, these decreases were even more pronounced. In the tested conditioned media of OCC, gelatin zymography revealed no proteolytic activity (*data not shown*). Altogether, these data show that extracellular MMC alters ECM protein production and organization by OCC.

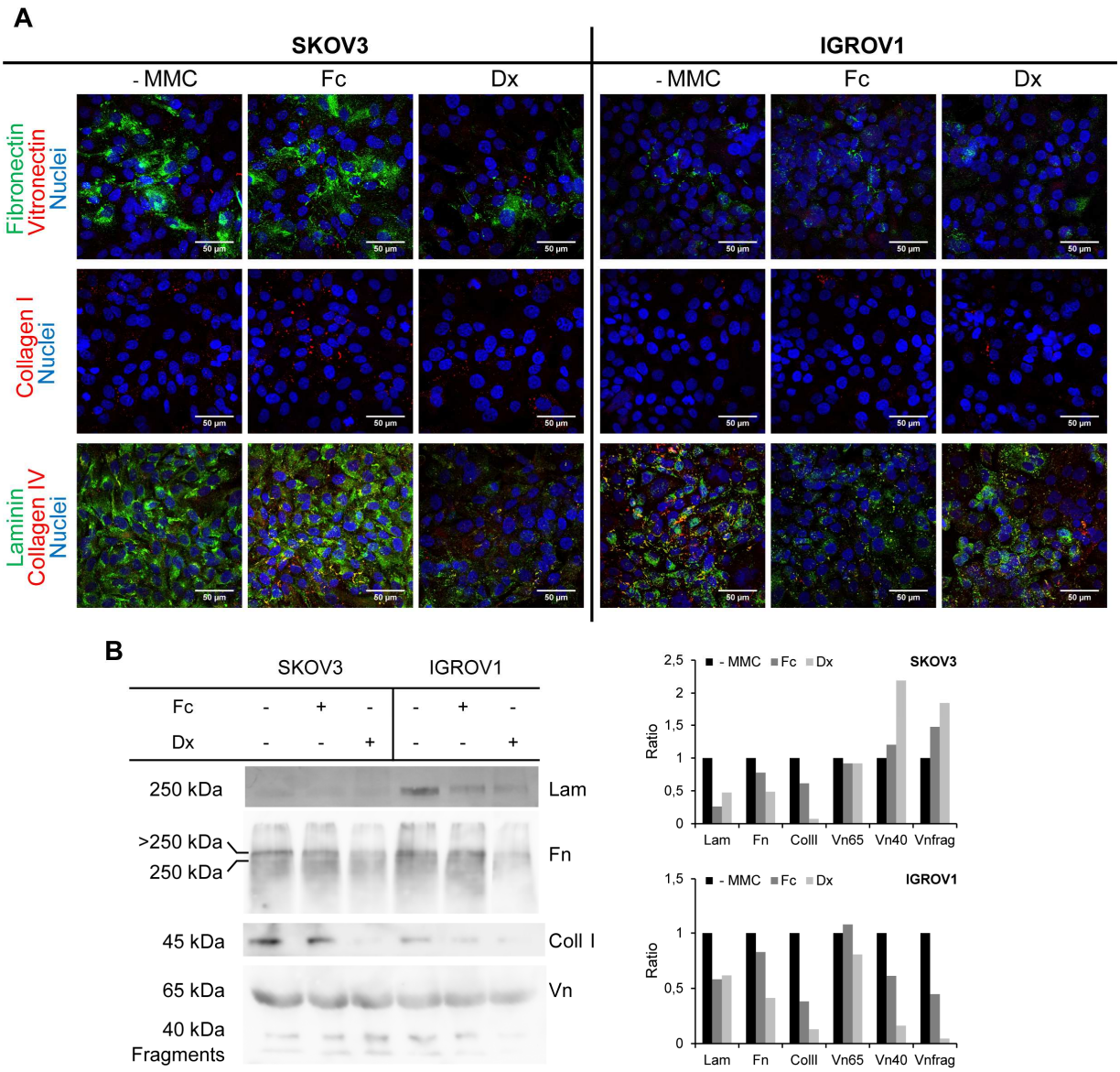

Figure 6. Extracellular macromolecular crowding alters OCC extracellular matrix organization. Adherent SKOV3 and IGROV1 cells were cultured 48h in their culture media supplemented with 0 (-MMC) or 75 mg/mL of Fc or Dx. (A) Stromal and basal ECM networks were then stained for fibronectin (Fn), vitronectin (Vn), collagen I (CollI), laminin (Lam), collagen IV, and nuclei. Representative images, of two independent experiments in duplicate, reveal decreased matrix deposition in presence of Dx. Scale bar: 50 µm. (B) Fn, Vn, CollI, and Lam in SKOV3 and IGROV1 cells growth medium cultured for 48h in the presence of 0 (-MMC) or 75 mg/mL of Fc or Dx were analyzed by western blot. Graphics represent the densitometric estimation of western blot. Quantification of western blot demonstrates that Fc and Dx decrease extracellular matrix proteins release in the supernatant.

Extracellular MMC affects the intracellular nucleus

To further elucidate the relationship between extracellular MMC on intracellular processes, we looked at the nucleus morphology. As shown in Table 1, SKOV3 and IGROV1 cells cultured with Fc had a similar mean nucleus area as their respective control cultured without MMC. However, when cultured with Dx, the mean nucleus area of cells increased significantly by about 15 and 11% respectively for SKOV3 and IGROV1 cells compared to the control. These results were confirmed by the analysis of the nucleus area distribution which correlated with

an increase of the nuclear shape index of SKOV3 and IGROV1 cells (Figure S6) [4]. These results witness of an effect of extracellular MMC on the intracellular nucleus, potentially impacting gene expression.

	SKOV3			IGROV1		
	- MMC	**Fc**	**Dx**	**- MMC**	**Fc**	**Dx**
Mean nucleus area (µm²)	**121,8 ± 9,4**	**117,8 ± 9**	**140,7 ± 11,9 *****	**103,6 ± 6,6**	**104,4 ± 5,7**	**114,8 ± 5,4 *****

Table 1. Extracellular macromolecular crowding impacts OCC intracellular nucleus area. Adherent SKOV3 and IGROV1 cells were cultured 48h in their culture media supplemented with 0 (-MMC) or 75 mg/mL of Fc or Dx. The mean nucleus area, represented as mean ± standard deviation, was quantified on more than 827 SKOV3 and 1512 IGROV1 nucleus of at least three independent experiments in duplicate. Significant differences were estimated by comparison to the control without crowders (-MMC) (***$p < 0.005$, Student's test) and demonstrated that Dx induces an increase in the nucleus area.

Discussion

In this study, we provide evidence that extracellular MMC could affect OCC behaviors during dissemination. Three previous studies worked on cancer cells associated with MMC. Sun *& al*. used MMC as a tool to extract nuclear protein from cancer cells [36]. Ranamukhaarachchi *& al.* mixed MMC to collagen to generate collagen gel with different architecture and study the tuning of breast cancer cells morphology and invasiveness [65]. Interestingly, Gonzalez *& al*. showed that crowders associated viscosity enhances liver cancer cells mechanosensing and migration [63]. Ovarian cancer is one of a kind where OCC is in direct contact with the biological fluid ascites from early stages. However, none of these studies looked at the effect of extracellular fluid MMC and its confinement on OCC. OCC disseminates through crucial steps: the growth of the primary tumor, shedding of cancer cells from the primary site into the peritoneal ascites, implantation to peritoneum to disseminate, and eventually dissemination through other body fluids like blood [9]. Ascites, and eventually blood, thus impact adherent OCC at the primary site, non-adherent OCC upon shedding, OCC implantation and re-adherent OCC upon implantation and dissemination. These two liquids are naturally crowded environments as they present high total protein concentration around 75 mg/mL and, are composed of high molecular weight molecules like fibronectin (200-250 kDa as a monomer and 400-500 kDa as a dimer) known to highly influence OCC [4,17,20,66,67]. As noted by Shadid *& al.*, to mimic MMC of biological fluids, the ideal crowding agent must provide a natural microenvironment [77]. Therefore, using ascites or blood would be the best approach. However, it would be difficult to interpret the experimental data due to their biochemical heterogeneity [19,78]. Indeed, Puiffe *& al.* remarkably showed that ovarian cancer cells OV-90 responses (in term of invasion, proliferation, spheroid formation, and gene expression) to different ascites is highly heterogeneous [79]. The study of Puiffe *& al.* also suggests a potential discriminatory effect on OCC between the biochemical and physical crowding properties of ascites when they heat-inactivate ascites. Therefore, we used a “bottom-up” reconstruction approach to mimic and understand MMC induced by high molecular weight molecules in fluids. We added either Fc 400 kDa or Dx 250 kDa, at the concentration of 75 mg/mL in cell culture media, a concentration representing the average total protein concentration estimated in human ovarian cancer ascites and blood. These two inert crowders, mimicking different high molecular weight biomolecules, have few similar biophysical features (charge and hydrodynamic radii). But they also present different features. Ribbon-like Dx presents a higher FVO compared to spheric Fc - 10 against 6.6% - which could differentially impact cell behaviors. FVO has previously been calculated for different proteins present in blood and was found to be ranging between 1.32 and 18.72 % witnessing the physiological relevance of our crowders concentration choice [70]. So here, a concentration of 75 mg/mL of crowders could mimic physiological MMC concentration and different physiological FVO. The influence of these two different kinds of crowders on OCC has then been investigated. The data suggested a differential OCC response depending on the cell phenotype and the crowders properties, especially the crowdedness represented by the FVO.

We looked at the impact of the two crowders on two OCC behaviors: SKOV3 cells with an intermediate-mesenchymal phenotype and IGROV1 cells with an intermediate-epithelial phenotype [3,73,74]. Fc did not affect the proliferation of either SKOV3 or IGROV1 cells, while Dx had a cytostatic effect without affecting

senescence but still promoting IGROV1 cell metabolic activity. In light of literature, MMC can have a versatile effect on cell proliferation. Indeed, MMC attenuated the proliferation of human adipose stem cells while it increased human fibroblasts and human bone marrow mesenchymal stem cell proliferation [70,80]. We have to note that our team previously showed that ascites do not impact SKOV3 and IGROV1 cell proliferation [3]. Thus, Fc acts similarly to ascites, while the higher crowding property of Dx seems to oppose biochemical cues of ascites and limit cell proliferation. The differential effect of Dx on cell metabolic activities indicates that SKOV3 and IGROV1 cells potentially use different metabolic pathways in crowded environments. Indeed, it has been revealed that quiescent cells redirect their metabolic activities from generating progeny to the preservation of self-integrity and alternative functions beneficial to the organism as a whole [81]. SKOV3 and IGROV1 cells could thus be using a similar strategy in crowded environments.

MMC impeded both SKOV3 and IGROV1 cell aggregation in spheroid. These results are opposite to the effect of ascites which promotes the compaction of SKOV3 and IGRVO1 spheroids [75]. These results also suggest that MMC hinders OCC aggregation and cell-cell adhesion probably by limiting the diffusion and sedimentation of cells. Indeed, many works showed that MMC reduces molecules diffusion and could thus also limit cell diffusion/sedimentation [28,31]. These results also highlight that MMC acts opposite of biochemical cues of ascites and that the biological molecules present in ascites like ECM proteins are probably major effectors for multicellular aggregation. Adding ECM proteins to crowded media could shed light on this aspect. For example, Lam and Fn, involved in spheroid maintenance, are known to be found in ovarian cancer ascites and are associated with malignant ovarian cancer and/or poor prognosis [82,83]. Interestingly, Burleson & al. showed that disaggregation of OCC spheroid is a helpful step for the colonization of mesothelial cell monolayers [84]. This suggests that MMC could be an advantageous property of fluid for OCC dissemination.

Upon shedding into biological body fluid, OCC implant to surrounding tissues in order to form metastasis. Our team showed that ascites would help OCC progression [3]. However here, beside cell-cell adhesion, extracellular MMC also hinders cell-substratum adhesion suggesting that MMC is an opposing force to ascites biochemical cues and to OCC implantation and dissemination. In the case of Fc, OCC adhesion presented a standard bell curve with a threshold concentration specific to each cell line and crowder. Low crowder concentration seems to increase cell adhesion. But high crowder concentration might generate steric hindrance and media density might become similar to cell density impeding cell sedimentation and adhesion.
In crowded environments, SKOV3 and IGROV1 cells reduced stress fibers and cortical actin to organize instead perinuclear actin fibers. These changes were more dramatic when cells were cultured with more crowding Dx. Cells switched to less adherent phenotype with less mature anchoring structures and, MMC promoted collective as well as individual migration patterns. This kind of change can happen in biochemically different environments. Our team previously showed that SKOV3 switched toward a more mesenchymal phenotype when cultured in ovarian cancer ascites or in the presence of amyloid-like fibronectin aggregates [3,4]. Here, we show that SKOV3 and IGROV1 cells can also switch phenotype upon different biophysical environments. Confinement and low adhesion can induce a fast amoeboid migration of mesenchymal cells [85]. Thus, we

could suppose that the confinement-like environment produced by extracellular MMC could emphasize more motile capacities of OCC. The study of Gonzalez-Molina *& al.* pointed in the same direction as our study as we both showed that MMC increases cancer cell migration [63]. Gonzalez-Molina *& al*. also highlighted that MMC induced mesenchymal migration was not always associated with an epithelial-mesenchymal transition switch. Cancer cells within a single tumor can simultaneously move collectively and individually [86]. Our results are a good example of coexisting migration patterns induced by MMC.

Here, we show for the first time that increased extracellular MMC could induce a more motile phenotype of OCC by a stabilization of ZO-1 and a potential translocation of E-cadherin in the nucleus in SKOV3 cells and, a decrease of intercellular E-cadherin in IGROV1 cells. Similar ZO-1 stabilization under crowded environments was previously described for stem cells [46]. Ilina *& al*. described the importance of ZO-1 for cell-cell interaction during collective migration [87]. Nuclear localization of E-cadherin with a concomitant loss of membrane E-cadherin has been found in several types of cancer and was systematically associated with accelerated tumor growth or increased migration, invasion, or aggressiveness [88–92]. Some studies showed that the cleaved E-cadherin fragment was translocated in the nucleus to increase tumor growth or prevent apoptosis [93,94]. Altogether the data suggest that MMC differentially promotes migration and dissemination of OCC with different junction protein organization mechanisms. This kind of junction protein reorganization is a well-known process during cell migration, and this reorganization can be different for each cell type [95].

In the overall work, attenuated cell-substratum and cell-cell adhesion in favor of accentuated migration in crowded environments seemed more prominent for SKOV3 cells compared to IGROV1 cells. This could be explained by their respective initial phenotype within the epithelial-mesenchymal spectrum: SKOV3 cells (isolated from ascites) present a mesenchymal-like phenotype, while IGROV1 cells (isolated from adenocarcinoma) have an epithelial-like phenotype and tend to form spontaneous spheroid. Indeed, it is important to note that while IGROV1 cells express αvβ3 integrin needed for directionally persistent migration, SKOV3 cells express both αvβ3 and αvβ5 integrins, the latest needed for collective migration [96–98]. A study showed that IGROV1 cells expressed E-cadherin while SKOV3 does not, and this was suggested in our experiments [73]. SKOV3 cells produce higher vimentin responsible for more invasive and less adhesive phenotype [99]. Gene and microRNA expression analysis showed that SKOV3 highly expressed genes involved in cell movement, invasion, and homing [100]. IGROV1 cells highly expressed genes involved in cell-cell adhesion [100]. Altogether, we suggest that the higher expression of genes implicated in adhesion, and especially E-cadherin, could explain the higher cell-cell and cell-substratum adhesion rate of IGROV1 cells in crowded environments. In the case of SKOV3 cells, the expression of migratory genes, especially integrins needed for migration with the stabilization of ZO-1 junctional protein needed for collective migration, could explain their lower adhesion and higher migration rate in crowded environments.

The more motile phenotype of OCC in crowded environments was associated with a decrease in stromal and basal ECM deposition, especially Fn and Lam matrix, and correlated with a decrease of their release in the

supernatant. In the case of intermediate-mesenchymal SKOV3 cells, Dx-associated crowding seemed to instigate the cleavage of Vn into smaller fragments. Altogether, these data indicate that MMC negatively impact protein production by OCC. We showed a similar effect on normal mesothelial Met5A cells which cover the peritoneal cavity. In this study, we looked solely at the effect of MMC on matrix deposition and not on matrix maturation. Indeed, type I collagen maturation requires ascorbic acid. Winter *& al.* showed that the combination of ascorbic acid with MMC helps to enhance collagen I matrix deposition by myometrial smooth muscle cells. It would be interesting to look at this combination on OCC [101]. While MMC has been widely studied for its property to accelerate ECM deposition by healthy cells and enhance tissue formation for tissue engineering, we here show that extracellular MMC can have an opposite effect in the case of OCC and mesothelial cells [50,52]. This could be explained by the differences in crowders properties especially concentration, size, and type of the crowder. This witnesses that MMC differentially affects ECM deposition and migration depending on the crowder properties.

It has greatly been shown that decellularized extracellular matrix produced in crowded environments helps either maintain the stemness of cells, maintain specialized cells like podocytes, or either drive stem cell differentiation [46,49,60]. This suggests that decellularized ECM produced in crowded environments could also fine-tune cancer fate. Besides, our results suggest that mesothelial ECM, an implantation site of OCC, is modified in crowded environment.

We showed that extracellular MMC has a direct effect on nucleus as its area increased. An increase in nuclear size was also observed in cervical cancer and high-grade urothelial carcinomas [102,103]. We can suppose that the reduced ECM protein production and deposition in crowded microenvironments could be a consequence of a decrease in intranuclear MMC and gene expression in a bigger nucleus. Indeed, the excessive increase of nucleus volume impairs cell-cycle progression by diluting the cyto- and nucleoplasm, decreasing intracellular MMC, and thus mRNA and protein expression not being proportional to the increased size [28,32,104–107]. But the increased size of the nucleus could also be explained by an accumulation of molecules in the nucleus like the observed E-cadherin in SKOV3 cells. Inhibition of nuclear export could also lead to an increase of nuclear size [108].

An increase of nuclear surface suggests a potential change in the force acting from the cytoplasm. So in crowded environments, the increased perinuclear actin at the expense of decreased cortical actin filament could be one of the driving forces of nuclear area increase. Indeed, several works showed that actin regulates nucleus morphology. The formation of perinuclear actin caps especially helps the flattening of the nucleus which seems to be the case in our experiments [109,110]. A study showed the increase of the nucleus projected area with the increased substrate stiffness [111]. As described by Liu & al., the cytoskeletal caging of the nucleus help to transmit the mechanical stresses that affect nuclear shape [26]. Actin filaments generate the forces that drive the nuclear movement through interconnections between the nuclear surface and the actin caps, which would prevent nuclear rotation and allow for nuclear translocation during migration. Altogether this suggests that in crowded environment nuclear caging by actin caps would help the translocation of nucleus during the migration. Further studies should be carried out to decipher lamin and

osmotic pressure involvement in nucleus size regulation in crowded environments [112,113]. The mechanisms regulating nucleus size in a crowded extracellular environment has to be further investigated in our model.

In the overall work, the results showed that, rather than the hydrodynamic radii of molecules, the FVO, thus the crowdedness, of the crowders seems to be important in regulating cell behaviors. The smaller the crowder is, the higher the FVO is and, the more drastic is the modification of OCC behaviors.

As future strategies, coupling the physical crowding property of fluid could change many perspectives in cancer model engineering and could be used as a more relevant model for drug screening or cancer studies. But this model could also be improved by taking into account several other parameters to fully understand the effect of extracellular MMC on OCC: concentration, molecular weight of crowder, mix of crowders, viscosity, crowder type, their charge, and their polydispersity [68]. So far, several studies have shown the effects of intracellular MMC but the direct relationship between extracellular MMC and intracellular activities like metabolism, gene expression and, vesicle transports in OCC is still unclear. In this study, we propose that MMC could be used to develop more relevant 3D *in vitro* models for cancer study. Highly performant microvasculature and microfluidic 3D *in vitro* model has already been developed [114]. Implementation of MMC in this model could help to understand the effect of MMC on cancer cells extravasation in an even more physiologically relevant model. Some studies showed the impact of MMC on collagen organization in hydrogels or on decellularized matrices for tissue-specific tailoring, and their subsequent effect on cell behaviors [56,60,65,115,116]. MMC and decellularized mesothelial matrix generated in crowded environments could be used as more relevant models for fundamental studies and drug screening assay integrating cancers cells behaviors on matrices and/or crowded environments [47,62]. As MMC seems to have a more important role in tuning OCC behaviors and ECM, it gives rise to a wide range of future possibilities to investigate ovarian cancer including cancer model engineering or drug screening.

Conclusions

The proposed study demonstrates that incorporating polymers of relevant macromolecular size and concentration into the extracellular liquid microenvironment could greatly influence OCC behaviors. We identified a differential role of MMC. While extracellular MMC negatively affects non-adherent OCC adhesion and aggregation; extracellular MMC promotes adherent OCC migration by decreasing ECM deposition and reorganizing the actin cytoskeleton and nucleus. Altogether, MMC promotes the dissemination phenotype of OCC. Moreover, the higher the crowdedness is, the more important is the effect of MMC on OCC behaviors, with a more impactful effect on mesenchymal-like OCC. MMC was shown to be a simple way to design a relevant biomimetic model of ovarian cancer integrating a biophysical property of fluids. This model can easily be tailored as a theoretical study tool to analyze implantation and dissemination of OCC through crowded biological fluids. It can also be used for tissue-specific matrix design with the purpose of cancer model engineering and drug screening.

Acknowledgments

We thank Mélanie Briand and Laurent Poulain from Biological Resources Centre "OvaRessources" (certified NF S 96-900, Cancer Center François Baclesse, Caen, France) for providing ascites samples used in this work. We thank Dr. Cedric Picot for graciously providing the senescence detection kit. We also thank Rémy Agniel and Lamia El Guermah for their help. Lastly, we thank the EA2526 LPPI unit (Laboratoire de Physicochimie des polymères et des interfaces, Cergy-Pontoise, France) for lending the Zetasizer.

Declaration of interest: none

Fundings

This research did not receive any specific grant from funding agencies in the public, commercial, or not-for-profit sectors.

Data availability

The raw/processed data required to reproduce these findings can be shared by the author upon request.

References

[1] J. Leroy-Dudal, C. Demeilliers, O. Gallet, E. Pauthe, S. Dutoit, R. Agniel, P. Gauduchon, F. Carreiras, Transmigration of human ovarian adenocarcinoma cells through endothelial extracellular matrix involves αv integrins and the participation of MMP2, Int. J. Cancer. 114 (2005) 531–543. doi:10.1002/ijc.20778.

[2] S. Kellouche, J. Fernandes, J. Leroy-Dudal, O. Gallet, S. Dutoit, L. Poulain, F. Carreiras, Initial formation of IGROV1 ovarian cancer multicellular aggregates involves vitronectin, Tumor Biol. 31 (2010) 129–139. doi:10.1007/s13277-010-0017-9.

[3] L. Carduner, J. Leroy-Dudal, C.R. Picot, O. Gallet, F. Carreiras, S. Kellouche, Ascites-induced shift along epithelial-mesenchymal spectrum in ovarian cancer cells: Enhancement of their invasive behavior partly dependant on αv integrins, Clin. Exp. Metastasis. 31 (2014) 675–688. doi:10.1007/s10585-014-9658-1.

[4] R. Bascetin, L. Blay, S. Kellouche, F. Carreiras, C.R. Picot, M. Briand, R. Agniel, O. Gallet, C. Vendrely, J. Leroy-Dudal, Fibronectin amyloid-like aggregation alters its extracellular matrix incorporation and promotes a single and sparsed cell migration, Exp. Cell Res. 371 (2018) 104–121. doi:10.1016/j.yexcr.2018.07.047.

[5] V. Prévost, K. David, P. Ferrandiz, O. Gallet, M. Hindié, Diffusions of sound frequencies designed to target dehydrins induce hydric stress tolerance in Pisum sativum seedings, Heliyon. 6 (2020) e04991. doi:10.1016/j.heliyon.2020.e04991.

[6] D.G. Tang, Understanding cancer stem cell heterogeneity and plasticity, Cell Res. 22 (2012) 457–472. doi:10.1038/cr.2012.13.

[7] M. Saxena, G. Christofori, Rebuilding cancer metastasis in the mouse, Mol. Oncol. 7 (2013) 283–296. doi:10.1016/j.molonc.2013.02.009.

[8] B. Emon, J. Bauer, Y. Jain, B. Jung, T. Saif, Biophysics of Tumor Microenvironment and Cancer Metastasis - A Mini Review, Comput. Struct. Biotechnol. J. 16 (2018) 279–287. doi:10.1016/j.csbj.2018.07.003.

[9] D.S. Tan, R. Agarwal, S.B. Kaye, Mechanisms of transcoelomic metastasis in ovarian cancer, Lancet Oncol. 7 (2006) 925–934. doi:10.1016/S1470-2045(06)70939-1.

[10] N.M. Moss, M. V. Barbolina, Y. Liu, L. Sun, H.G. Munshi, M.S. Stack, Ovarian cancer cell detachment and multicellular aggregate formation are regulated by membrane type 1 matrix metalloproteinase: A potential role in I.p. metastatic dissemination, Cancer Res. 69 (2009) 7121–7129. doi:10.1158/0008-5472.CAN-08-4151.

[11] N.A. Chebotareva, B.I. Kurganov, N.B. Livanova, Biochemical effects of molecular crowding, Biochem. 69 (2004) 1239–1251. doi:10.1007/s10541-005-0070-y.

[12] A.S. Zeiger, F.C. Loe, R. Li, M. Raghunath, K.J. van Vliet, Macromolecular crowding directs

extracellular matrix organization and mesenchymal stem cell behavior, PLoS One. 7 (2012). doi:10.1371/journal.pone.0037904.

[13] I.M. Kuznetsova, K.K. Turoverov, V.N. Uversky, What macromolecular crowding can do to a protein, 2014. doi:10.3390/ijms151223090.

[14] S.B. Zimmerman, S.O. Trach, Estimation of macromolecule concentrations and excluded volume effects for the cytoplasm of Escherichia coli, J. Mol. Biol. 222 (1991) 599–620. doi:10.1016/0022-2836(91)90499-V.

[15] J.R. Daban, Physical constraints in the condensation of eukaryotic chromosomes. Local concentration of DNA versus linear packing ratio in higher order chromatin structures, Biochemistry. 39 (2000) 3861–3866. doi:10.1021/bi992628w.

[16] B. Bohrmann, M. Haider, E. Kellenberger, Concentration evaluation of chromatin in unstained resin-embedded sections by means of low-dose ratio-contrast imaging in STEM, Ultramicroscopy. 49 (1993) 235–251. doi:10.1016/0304-3991(93)90230-U.

[17] B. Okutucu, A. Dinçer, Ö. Habib, F. Zihnioglu, Comparison of five methods for determination of total plasma protein concentration, J. Biochem. Biophys. Methods. 70 (2007) 709–711. doi:10.1016/j.jbbm.2007.05.009.

[18] R.O. Hynes, A. Naba, Overview of the matrisome-An inventory of extracellular matrix constituents and functions, Cold Spring Harb. Perspect. Biol. 4 (2012) a004903. doi:10.1101/cshperspect.a004903.

[19] E. Kipps, D.S.P. Tan, S.B. Kaye, Meeting the challenge of ascites in ovarian cancer: new avenues for therapy and research., Nat. Rev. Cancer. 13 (2013) 273–82. doi:10.1038/nrc3432.

[20] A.P. Lucas Oliveira, Proteomic Analysis of Ovarian Cancer Tumor Fluid is a Rich Source of Potential Biomarkers, J. Proteomics Bioinform. s5 (2015) 4. doi:10.4172/jpb.s5-004.

[21] L. Wang, C. Wang, S. Wu, Y. Fan, X. Li, Influence of the mechanical properties of biomaterials on degradability, cell behaviors and signaling pathways: current progress and challenges, Biomater. Sci. 8 (2020) 2714–2733. doi:10.1039/d0bm00269k.

[22] D. Huber, A. Oskooei, X. Casadevall Solvas, Andrew Demello, G. V. Kaigala, Hydrodynamics in Cell Studies, Chem. Rev. 118 (2018) 2042–2079. doi:10.1021/acs.chemrev.7b00317.

[23] M. Huang, S. Fan, W. Xing, C. Liu, Microfluidic cell culture system studies and computational fluid dynamics, Math. Comput. Model. 52 (2010) 2036–2042. doi:10.1016/j.mcm.2010.01.024.

[24] J.A. Nagy, M.S. Meyers, E.M. Masse, K.T. Herzberg, H.F. Dvorak, Pathogenesis of Ascites Tumor Growth: Fibrinogen Influx and Fibrin Accumulation in Tissues Lining the Peritoneal Cavity, Cancer Res. 55 (1995).

[25] R. Chapanian, D.H. Kwan, I. Constantinescu, F.A. Shaikh, N.A.A. Rossi, S.G. Withers, J.N. Kizhakkedathu, Enhancement of biological reactions on cell surfaces via macromolecular

crowding, Nat. Commun. 5 (2014) 4683. doi:10.1038/ncomms5683.

[26] N. Muramatsu, A.P. Minton, Tracer diffusion of globular proteins in concentrated protein solutions., Proc. Natl. Acad. Sci. 85 (2006) 2984–2988. doi:10.1073/pnas.85.9.2984.

[27] A.P. Minton, Molecular crowding: Analysis of effects of high concentrations of inert cosolutes on biochemical equilibria and rates in terms of volume exclusion, Methods Enzymol. 295 (1998) 127–149. doi:10.1016/S0076-6879(98)95038-8.

[28] A. Bancaud, S. Huet, N. Daigle, J. Mozziconacci, J. Beaudouin, J. Ellenberg, Molecular crowding affects diffusion and binding of nuclear proteins in heterochromatin and reveals the fractal organization of chromatin, EMBO J. 28 (2009) 3785–3798. doi:10.1038/emboj.2009.340.

[29] K. Richter, M. Nessling, P. Lichter, Experimental evidence for the influence of molecular crowding on nuclear architecture, J. Cell Sci. 120 (2007) 1673–1680. doi:10.1242/jcs.03440.

[30] K. Richter, M. Nessling, P. Lichter, Macromolecular crowding and its potential impact on nuclear function, Biochim. Biophys. Acta - Mol. Cell Res. 1783 (2008) 2100–2107. doi:10.1016/j.bbamcr.2008.07.017.

[31] C. Tan, S. Saurabh, M.P. Bruchez, R. Schwartz, P. Leduc, Molecular crowding shapes gene expression in synthetic cellular nanosystems, Nat. Nanotechnol. 8 (2013) 602–608. doi:10.1038/nnano.2013.132.

[32] M. Golkaram, S. Hellander, B. Drawert, L.R. Petzold, Macromolecular Crowding Regulates the Gene Expression Profile by Limiting Diffusion., PLoS Comput. Biol. 12 (2016) e1005122. doi:10.1371/journal.pcbi.1005122.

[33] A. Miermont, F. Waharte, S. Hu, M.N. McClean, S. Bottani, S. Leon, P. Hersen, Severe osmotic compression triggers a slowdown of intracellular signaling, which can be explained by molecular crowding, Proc. Natl. Acad. Sci. 110 (2013) 5725–5730. doi:10.1073/pnas.1215367110.

[34] P. Nunes, I. Roth, P. Meda, E. Féraille, D. Brown, U. Hasler, Ionic imbalance, in addition to molecular crowding, abates cytoskeletal dynamics and vesicle motility during hypertonic stress, Proc. Natl. Acad. Sci. 112 (2015) E3104–E3113. doi:10.1073/pnas.1421290112.

[35] R. Rashid, S.M.L. Chee, M. Raghunath, T. Wohland, Macromolecular crowding gives rise to microviscosity, anomalous diffusion and accelerated actin polymerization, Phys. Biol. 12 (2015) 034001. doi:10.1088/1478-3975/12/3/034001.

[36] L. Sun, J. Fang, Macromolecular crowding effect is critical for maintaining SIRT1's nuclear localization in cancer cells, Cell Cycle. 15 (2016) 2647–2655. doi:10.1080/15384101.2016.1211214.

[37] A. Vazquez, Z.N. Oltvai, Molecular crowding defines a common origin for the warburg effect in proliferating cells and the lactate threshold in muscle physiology, PLoS One. 6 (2011) e19538.

doi:10.1371/journal.pone.0019538.

[38] K. Burkewitz, K. Choe, K. Strange, Hypertonic stress induces rapid and widespread protein damage in C. elegans, Am. J. Physiol. Physiol. 301 (2011) C566–C576. doi:10.1152/ajpcell.00030.2011.

[39] A. Vazquez, Metabolic States Following Accumulation of Intracellular Aggregates: Implications for Neurodegenerative Diseases, PLoS One. 8 (2013) e63822. doi:10.1371/journal.pone.0063822.

[40] S. Mittal, R.K. Chowhan, L.R. Singh, Macromolecular crowding: Macromolecules friend or foe, Biochim. Biophys. Acta - Gen. Subj. 1850 (2015) 1822–1831. doi:10.1016/J.BBAGEN.2015.05.002.

[41] Y.Q. Fan, H.J. Liu, C. Li, Y.S. Luan, J.M. Yang, Y.L. Wang, Effects of macromolecular crowding on refolding of recombinant human brain-type creatine kinase, Int. J. Biol. Macromol. 51 (2012) 113–118. doi:10.1016/j.ijbiomac.2012.04.014.

[42] D.M. Hatters, A.P. Minton, G.J. Howlett, Macromolecular crowding accelerates amyloid formation by human apolipoprotein C-II, J. Biol. Chem. 277 (2002) 7824–7830. doi:10.1074/jbc.M110429200.

[43] B. Ma, J. Xie, L. Wei, W. Li, Macromolecular crowding modulates the kinetics and morphology of amyloid self-assembly by β-lactoglobulin, Int. J. Biol. Macromol. 53 (2013) 82–87. doi:10.1016/j.ijbiomac.2012.11.008.

[44] G.A. Siddiqui, A. Naeem, Aggregation of globular protein as a consequences of macromolecular crowding: A time and concentration dependent study, Int. J. Biol. Macromol. 108 (2018) 360–366. doi:10.1016/j.ijbiomac.2017.12.001.

[45] A. Sohail, S.A. Bhat, A.A. Siddiqui, M. Zaman, R.H. Khan, B. Bano, Conformational transitions induced by in vitro macromolecular crowding lead to the amyloidogenesis of buffalo heart cystatin, J. Mol. Recognit. 28 (2015) 699–709. doi:10.1002/jmr.2484.

[46] S. McLenachan, E. Hao, D. Zhang, L. Zhang, M. Edel, F. Chen, Bioengineered Bruch's-like extracellular matrix promotes retinal pigment epithelial differentiation, Biochem. Biophys. Reports. 10 (2017) 178–185. doi:10.1016/j.bbrep.2017.03.008.

[47] C.Z.C. Chen, Y.X. Peng, Z.B. Wang, P. V Fish, J.L. Kaar, R.R. Koepsel, A.J. Russell, R.R. Lareu, M. Raghunath, The Scar-in-a-Jar: Studying potential antifibrotic compounds from the epigenetic to extracellular level in a single well, Br. J. Pharmacol. 158 (2009) 1196–1209. doi:10.1111/j.1476-5381.2009.00387.x.

[48] R.R. Lareu, K.H. Subramhanya, Y. Peng, P. Benny, C. Chen, Z. Wang, R. Rajagopalan, M. Raghunath, Collagen matrix deposition is dramatically enhanced in vitro when crowded with charged macromolecules: The biological relevance of the excluded volume effect, FEBS Lett.

581 (2007) 2709–2714. doi:10.1016/j.febslet.2007.05.020.

[49] Y. Peng, M.T. Bocker, J. Holm, W.S. Toh, C.S. Hughes, F. Kidwai, G.A. Lajoie, T. Cao, F. Lyko, M. Raghunath, Human fibroblast matrices bio-assembled under macromolecular crowding support stable propagation of human embryonic stem cells, J. Tissue Eng. Regen. Med. 6 (2012) e74–e86. doi:10.1002/term.1560.

[50] A. Satyam, P. Kumar, X. Fan, A. Gorelov, Y. Rochev, L. Joshi, H. Peinado, D. Lyden, B. Thomas, B. Rodriguez, M. Raghunath, A. Pandit, D. Zeugolis, Macromolecular Crowding Meets Tissue Engineering by Self-Assembly: A Paradigm Shift in Regenerative Medicine, Adv. Mater. 26 (2014) 3024–3034. doi:10.1002/adma.201304428.

[51] A. Satyam, P. Kumar, D. Cigognini, A. Pandit, D.I. Zeugolis, Low, but not too low, oxygen tension and macromolecular crowding accelerate extracellular matrix deposition in human dermal fibroblast culture, Acta Biomater. 44 (2016) 221–231. doi:10.1016/j.actbio.2016.08.008.

[52] X.M. Ang, M.H.C. Lee, A. Blocki, C. Chen, L.L.S. Ong, H.H. Asada, A. Sheppard, M. Raghunath, Macromolecular Crowding Amplifies Adipogenesis of Human Bone Marrow-Derived Mesenchymal Stem Cells by Enhancing the Pro-Adipogenic Microenvironment, Tissue Eng. Part A. 20 (2013) 966–981. doi:10.1089/ten.tea.2013.0337.

[53] D. Cigognini, D. Gaspar, P. Kumar, A. Satyam, S. Alagesan, C. Sanz-Nogués, M. Griffin, T. O'Brien, A. Pandit, D.I. Zeugolis, Macromolecular crowding meets oxygen tension in human mesenchymal stem cell culture - A step closer to physiologically relevant in vitro organogenesis, Sci. Rep. 6 (2016) 30746. doi:10.1038/srep30746.

[54] R.R. Lareu, I. Arsianti, H.K. Subramhanya, P. Yanxian, M. Raghunath, In vitro enhancement of collagen matrix formation and crosslinking for applications in tissue engineering: A preliminary study, Tissue Eng. 13 (2007) 385–391. doi:10.1089/ten.2006.0224.

[55] C. Chen, F. Loe, A. Blocki, Y. Peng, M. Raghunath, Applying macromolecular crowding to enhance extracellular matrix deposition and its remodeling in vitro for tissue engineering and cell-based therapies, Adv. Drug Deliv. Rev. 63 (2011) 277–290. doi:10.1016/j.addr.2011.03.003.

[56] J.-Y. Dewavrin, N. Hamzavi, V.P.W. Shim, M. Raghunath, Tuning the architecture of three-dimensional collagen hydrogels by physiological macromolecular crowding, Acta Biomater. 10 (2014) 4351–4359. doi:10.1016/J.ACTBIO.2014.06.006.

[57] J.Y. Dewavrin, M. Abdurrahiem, A. Blocki, M. Musib, F. Piazza, M. Raghunath, Synergistic rate boosting of collagen fibrillogenesis in heterogeneous mixtures of crowding agents, J. Phys. Chem. B. 119 (2015) 4350–4358. doi:10.1021/jp5077559.

[58] M. Assunção, C.W. Wong, J.J. Richardson, R. Tsang, S. Beyer, M. Raghunath, A. Blocki,

Macromolecular dextran sulfate facilitates extracellular matrix deposition by electrostatic interaction independent from a macromolecular crowding effect, Mater. Sci. Eng. C. 106 (2020) 110280. doi:10.1016/j.msec.2019.110280.

[59] M.C. Prewitz, A. Stißel, J. Friedrichs, N. Träber, S. Vogler, M. Bornhäuser, C. Werner, Extracellular matrix deposition of bone marrow stroma enhanced by macromolecular crowding, Biomaterials. 73 (2015) 60–69. doi:10.1016/j.biomaterials.2015.09.014.

[60] A. Satyam, M.G. Tsokos, J.S. Tresback, D.I. Zeugolis, G.C. Tsokos, Cell-Derived Extracellular Matrix-Rich Biomimetic Substrate Supports Podocyte Proliferation, Differentiation, and Maintenance of Native Phenotype, Adv. Funct. Mater. (2020) 1908752. doi:10.1002/adfm.201908752.

[61] N. L'Heureux, N. Dusserre, G. Konig, B. Victor, P. Keire, T.N. Wight, N.A.F. Chronos, A.E. Kyles, C.R. Gregory, G. Hoyt, R.C. Robbins, T.N. McAllister, Human tissue-engineered blood vessels for adult arterial revascularization, Nat. Med. 12 (2006) 361–365. doi:10.1038/nm1364.

[62] M. Graupp, H.-J. Gruber, G. Weiss, K. Kiesler, S. Bachna-Rotter, G. Friedrich, M. Gugatschka, Establishing principles of macromolecular crowding for in vitro fibrosis research of the vocal fold lamina propria, Laryngoscope. 125 (2015) E203–E209. doi:10.1002/lary.25103.

[63] J. Gonzalez-Molina, X. Zhang, M. Borghesan, J. Mendonça da Silva, M. Awan, B. Fuller, N. Gavara, C. Selden, Extracellular fluid viscosity enhances liver cancer cell mechanosensing and migration, Biomaterials. 177 (2018) 113–124. doi:10.1016/j.biomaterials.2018.05.058.

[64] J. Gonzalez-Molina, J. Mendonça da Silva, B. Fuller, C. Selden, The extracellular fluid macromolecular composition differentially affects cell-substrate adhesion and cell morphology, Sci. Rep. 9 (2019) 8505. doi:10.1038/s41598-019-44960-3.

[65] S.K. Ranamukhaarachchi, R.N. Modi, A. Han, D.O. Velez, A. Kumar, A.J. Engler, S.I. Fraley, Macromolecular crowding tunes 3D collagen architecture and cell morphogenesis, Biomater. Sci. 7 (2019) 618–633. doi:10.1039/c8bm01188e.

[66] L. Poulouin, O. Gallet, M. Rouahi, J.M. Imhoff, Plasma fibronectin: three steps to purification and stability., Protein Expr. Purif. 17 (1999) 146–152. doi:10.1006/prep.1999.1103.

[67] L. Carduner, R. Agniel, S. Kellouche, C.R. Picot, C. Blanc-Fournier, J. Leroy-Dudal, F. Carreiras, Ovarian cancer ascites-derived vitronectin and fibronectin: Combined purification, molecular features and effects on cell response, Biochim. Biophys. Acta - Gen. Subj. 1830 (2013) 4885–4897. doi:10.1016/j.bbagen.2013.06.023.

[68] D. Gaspar, K.P. Fuller, D.I. Zeugolis, Polydispersity and negative charge are key modulators of extracellular matrix deposition under macromolecular crowding conditions, Acta Biomater. 88 (2019) 197–210. doi:10.1016/J.ACTBIO.2019.02.050.

[69] K.S. HARVE, M. RAGHUNATH, R.R. LAREU, R. RAJAGOPALAN, MACROMOLECULAR CROWDING

IN BIOLOGICAL SYSTEMS: DYNAMIC LIGHT SCATTERING (DLS) TO QUANTIFY THE EXCLUDED VOLUME EFFECT (EVE), Biophys. Rev. Lett. 01 (2006) 317–325. doi:10.1142/s1793048006000215.

[70] R. Rashid, N.S.J. Lim, S.M.L. Chee, S.N. Png, T. Wohland, M. Raghunath, Novel Use for Polyvinylpyrrolidone as a Macromolecular Crowder for Enhanced Extracellular Matrix Deposition and Cell Proliferation, Tissue Eng. Part C Methods. 20 (2014) 994–1002. doi:10.1089/ten.tec.2013.0733.

[71] C.F. Lee, S. Bird, M. Shaw, L. Jean, D.J. Vaux, Combined effects of agitation, macromolecular crowding, and interfaces on amyloidogenesis, J. Biol. Chem. 287 (2012) 38006–38019. doi:10.1074/jbc.M112.400580.

[72] G. Sahagun, S.A. Moore, M.N. Hart, Permeability of neutral vs. anionic dextrans in cultured brain microvascular endothelium, Am. J. Physiol. Circ. Physiol. 259 (2017) H162–H166. doi:10.1152/ajpheart.1990.259.1.h162.

[73] R.Y.J. Huang, M.K. Wong, T.Z. Tan, K.T. Kuay, A.H. C Ng, V.Y. Chung, Y.S. Chu, N. Matsumura, H.C. Lai, Y.F. Lee, W.J. Sim, C. Chai, E. Pietschmann, S. Mori, J.J.H. Low, M. Choolani, J.P. Thiery, An EMT spectrum defines an anoikis-resistant and spheroidogenic intermediate mesenchymal state that is sensitive to e-cadherin restoration by a src-kinase inhibitor, saracatinib (AZD0530), Cell Death Dis. 4 (2013) e915–e915. doi:10.1038/cddis.2013.442.

[74] M. Rosso, B. Majem, L. Devis, L. Lapyckyj, M.J. Besso, M. Llauradó, M.F. Abascal, M.L. Matos, L. Lanau, J. Castellví, J.L. Sánchez, A. Pérez Benavente, A. Gil-Moreno, J. Reventós, A. Santamaria Margalef, M. Rigau, M.H. Vazquez-Levin, E-cadherin: A determinant molecule associated with ovarian cancer progression, dissemination and aggressiveness, PLoS One. 12 (2017) e0184439. doi:10.1371/journal.pone.0184439.

[75] K.L. Sodek, K.J. Murphy, T.J. Brown, M.J. Ringuette, Cell–cell and cell–matrix dynamics in intraperitoneal cancer metastasis, Cancer Metastasis Rev. 31 (2012) 397–414. doi:10.1007/s10555-012-9351-2.

[76] C.M. Niessen, Tight Junctions/Adherens Junctions: Basic Structure and Function, J. Invest. Dermatol. 127 (2007) 2525–2532. doi:10.1038/SJ.JID.5700865.

[77] S. Shahid, M.I. Hassan, A. Islam, F. Ahmad, Size-dependent studies of macromolecular crowding on the thermodynamic stability, structure and functional activity of proteins: in vitro and in silico approaches, Biochim. Biophys. Acta - Gen. Subj. 1861 (2017) 178–197. doi:10.1016/j.bbagen.2016.11.014.

[78] I. Matte, D. Lane, C. Laplante, C. Rancourt, A. Piché, Profiling of cytokines in human epithelial ovarian cancer ascites., Am. J. Cancer Res. 2 (2012) 566–80. http://www.ncbi.nlm.nih.gov/pubmed/22957308 (accessed June 30, 2018).

[79] M.L. Puiffe, C. Le Page, A. Filali-Mouhim, M. Zietarska, V. Ouellet, P.N. Tonin, M. Chevrette, D.M. Provencher, A.M. Mes-Masson, Characterization of ovarian cancer ascites on cell invasion, proliferation, spheroid formation, and gene expression in an in vitro model of epithelial ovarian cancer, Neoplasia. 9 (2007) 820–829. doi:10.1593/neo.07472.

[80] M. Patrikoski, M.H.C. Lee, L. Mäkinen, X.M. Ang, B. Mannerström, M. Raghunath, S. Miettinen, Effects of Macromolecular Crowding on Human Adipose Stem Cell Culture in Fetal Bovine Serum, Human Serum, and Defined Xeno-Free/Serum-Free Conditions, Stem Cells Int. 2017 (2017) 1–14. doi:10.1155/2017/6909163.

[81] J.M.S. Lemons, H.A. Coller, X.J. Feng, B.D. Bennett, A. Legesse-Miller, E.L. Johnson, I. Raitman, E.A. Pollina, H.A. Rabitz, J.D. Rabinowitz, Quiescent fibroblasts exhibit high metabolic activity, PLoS Biol. 8 (2010). doi:10.1371/journal.pbio.1000514.

[82] J.M. Santos, S.P. Camões, E. Filipe, M. Cipriano, R.N. Barcia, M. Filipe, M. Teixeira, S. Simões, M. Gaspar, D. Mosqueira, D.S. Nascimento, P. Pinto-do-Ó, P. Cruz, H. Cruz, M. Castro, J.P. Miranda, Three-dimensional spheroid cell culture of umbilical cord tissue-derived mesenchymal stromal cells leads to enhanced paracrine induction of wound healing, Stem Cell Res. Ther. 6 (2015) 90. doi:10.1186/s13287-015-0082-5.

[83] A. Cho, V.M. Howell, E.K. Colvin, The Extracellular Matrix in Epithelial Ovarian Cancer - A Piece of a Puzzle., Front. Oncol. 5 (2015) 245. doi:10.3389/fonc.2015.00245.

[84] K. Burleson, M. Boente, S. Pambuccian, A. Skubitz, Disaggregation and invasion of ovarian carcinoma ascites spheroids., J. Transl. Med. 4 (2006) 6. doi:10.1186/1479-5876-4-6.

[85] Y.-J. Liu, M. Le Berre, F. Lautenschlaeger, P. Maiuri, A. Callan-Jones, M. Heuzé, T. Takaki, R. Voituriez, M. Piel, Confinement and Low Adhesion Induce Fast Amoeboid Migration of Slow Mesenchymal Cells, Cell. 160 (2015) 659–672. doi:10.1016/J.CELL.2015.01.007.

[86] N. V Krakhmal, M. V Zavyalova, E. V Denisov, S. V Vtorushin, V.M. Perelmuter, Cancer Invasion: Patterns and Mechanisms., Acta Naturae. 7 (2015) 17–28. http://www.ncbi.nlm.nih.gov/pubmed/26085941 (accessed August 3, 2019).

[87] O. Ilina, P. Friedl, Mechanisms of collective cell migration at a glance, J. Cell Sci. 122 (2009) 3203–3208. doi:10.1242/jcs.036525.

[88] Y. Zhao, T. Yu, N. Zhang, J. Chen, P. Zhang, S. Li, L. Luo, Z. Cui, Y. Qin, F. Liu, Nuclear E-Cadherin Acetylation Promotes Colorectal Tumorigenesis via Enhancing β-Catenin Activity., Mol. Cancer Res. 17 (2019) 655–665. doi:10.1158/1541-7786.MCR-18-0637.

[89] S. Serra, S. Salahshor, M. Fagih, F. Niakosari, J.M. Radhi, R. Chetty, Nuclear expression of E-Cadherin in solid pseudopapillary tumors of the pancreas, J. Pancreas. 8 (2007) 296–303. http://pancreas.imedpub.com/nuclear-expression-of-ecadherin-in-solid-pseudopapillary-tumors-of-the-pancreas.php?aid=2643 (accessed July 14, 2019).

[90] M.S. Elston, A.J. Gill, J. V. Conaglen, A. Clarkson, R.J. Cook, N.S. Little, B.G. Robinson, R.J. Clifton-Bligh, K.L. McDonald, Nuclear accumulation of E-Cadherin correlates with loss of cytoplasmic membrane staining and invasion in pituitary adenomas, J. Clin. Endocrinol. Metab. 94 (2009) 1436–1442. doi:10.1210/jc.2008-2075.

[91] A.C. Han, A.P. Soler, C.K. Tang, K.A. Knudsen, H. Salazar, Nuclear localization of E-cadherin expression in Merkel cell carcinoma., Arch. Pathol. Lab. Med. 124 (2000) 1147–51. doi:10.1043/0003-9985(2000)124<1147:NLOECE>2.0.CO;2.

[92] M. Barshishat, S. Polak-Charcon, B. Schwartz, Butyrate regulates E-cadherin transcription, isoform expression and intracellular position in colon cancer cells, Br. J. Cancer. 82 (2002) 195–203. doi:10.1054/bjoc.1999.0899.

[93] M.V. Céspedes, M.J. Larriba, M.A. Pavón, P. Álamo, I. Casanova, M. Parreño, A. Feliu, F.J. Sancho, A. Muñoz, R. Mangues, Site-dependent E-cadherin cleavage and nuclear translocation in a metastatic colorectal cancer model, Am. J. Pathol. 177 (2010) 2067–2079. doi:10.2353/ajpath.2010.100079.

[94] E.C. Ferber, M. Kajita, A. Wadlow, L. Tobiansky, C. Niessen, H. Ariga, J. Daniel, Y. Fujita, A role for the cleaved cytoplasmic domain of E-cadherin in the nucleus, J. Biol. Chem. 283 (2008) 12691–12700. doi:10.1074/jbc.M708887200.

[95] S. Etienne-Manneville, Polarity proteins in migration and invasion, Oncogene. 27 (2008) 6970–6980. doi:10.1038/onc.2008.347.

[96] S. Cruet-Hennequart, S. Maubant, J. Luis, P. Gauduchon, C. Staedel, S. Dedhar, αv integrins regulate cell proliferation through integrin-linked kinase (ILK) in ovarian cancer cells, Oncogene. 22 (2003) 1688–1702. doi:10.1038/sj.onc.1206347.

[97] R.J. Petrie, A.D. Doyle, K.M. Yamada, Random versus directionally persistent cell migration, Nat. Rev. Mol. Cell Biol. 10 (2009) 538–549. doi:10.1038/nrm2729.

[98] S.N. Lee, J.S. Ahn, S.G. Lee, H.S. Lee, A.M.K. Choi, J.H. Yoon, Integrins α v5 and avb6 mediate IL-4-induced collective migration in human airway epithelial cells, Am. J. Respir. Cell Mol. Biol. 60 (2019) 420–433. doi:10.1165/rcmb.2018-0081OC.

[99] D. Fang, H. Chen, J.Y. Zhu, W. Wang, Y. Teng, H.-F. Ding, Q. Jing, S.-B. Su, S. Huang, Epithelial-mesenchymal transition of ovarian cancer cells is sustained by Rac1 through simultaneous activation of MEK1/2 and Src signaling pathways., Oncogene. 36 (2017) 1546–1558. doi:10.1038/onc.2016.323.

[100] C.M. Beaufort, J.C.A. Helmijr, A.M. Piskorz, M. Hoogstraat, K. Ruigrok-Ritstier, N. Besselink, M. Murtaza, W.F.J. van IJcken, A.A.J. Heine, M. Smid, M.J. Koudijs, J.D. Brenton, E.M.J.J. Berns, J. Helleman, Ovarian Cancer Cell Line Panel (OCCP): Clinical Importance of In Vitro Morphological Subtypes, PLoS One. 9 (2014) e103988. doi:10.1371/journal.pone.0103988.

[101] A. Winter, L.A. Salamonsen, J. Evans, Modelling fibroid pathology: development and manipulation of a myometrial smooth muscle cell macromolecular crowding model to alter extracellular matrix deposition, Mol. Hum. Reprod. (n.d.). doi:10.1093/MOLEHR/GAAA036.

[102] D.N. Slater, S. Rice, R. Stewart, S.E. Melling, E.M. Hewer, J.H.F. Smith, Proposed Sheffield quantitative criteria in cervical cytology to assist the grading of squamous cell dyskaryosis, as the British Society for Clinical Cytology definitions require amendment, Cytopathology. 16 (2005) 179–192. doi:10.1111/j.1365-2303.2005.00271.x.

[103] K. Poropatich, J.C. Yang, R. Goyal, V. Parini, X.J. Yang, Nuclear size measurement for distinguishing urothelial carcinomas from reactive urothelium on tissue sections, Diagn. Pathol. 11 (2016) 57. doi:10.1186/s13000-016-0501-7.

[104] J. Fidorra, T. Mielke, J. Booz, L.E. Feinendegen, Cellular and nuclear volume of human cells during the cell cycle, Radiat. Environ. Biophys. 19 (1981) 205–214. doi:10.1007/BF01324188.

[105] J.G. Umen, The elusive sizer, Curr. Opin. Cell Biol. 17 (2005) 435–441. doi:10.1016/J.CEB.2005.06.001.

[106] G.E. Neurohr, R.L. Terry, J. Lengefeld, M. Bonney, G.P. Brittingham, F. Moretto, T.P. Miettinen, L.P. Vaites, L.M. Soares, J.A. Paulo, J.W. Harper, S. Buratowski, S. Manalis, F.J. van Werven, L.J. Holt, A. Amon, Excessive Cell Growth Causes Cytoplasm Dilution And Contributes to Senescence, Cell. 176 (2019) 1083-1097.e18. doi:10.1016/j.cell.2019.01.018.

[107] R. Hancock, A role for macromolecular crowding effects in the assembly and function of compartments in the nucleus, J. Struct. Biol. 146 (2004) 281–290. doi:10.1016/J.JSB.2003.12.008.

[108] F.R. Neumann, P. Nurse, Nuclear size control in fission yeast., J. Cell Biol. 179 (2007) 593–600. doi:10.1083/jcb.200708054.

[109] S.B. Khatau, C.M. Hale, P.J. Stewart-Hutchinson, M.S. Patel, C.L. Stewart, P.C. Searson, D. Hodzic, D. Wirtz, A perinuclear actin cap regulates nuclear shape, Proc. Natl. Acad. Sci. U. S. A. 106 (2009) 19017–19022. doi:10.1073/pnas.0908686106.

[110] J.K. Kim, A. Louhghalam, G. Lee, B.W. Schafer, D. Wirtz, D.H. Kim, Nuclear lamin A/C harnesses the perinuclear apical actin cables to protect nuclear morphology, Nat. Commun. 8 (2017) 1–13. doi:10.1038/s41467-017-02217-5.

[111] R. Vishavkarma, S. Raghavan, C. Kuyyamudi, A. Majumder, J. Dhawan, P.A. Pullarkat, Role of actin filaments in correlating nuclear shape and cell spreading, PLoS One. 9 (2014) 107895. doi:10.1371/journal.pone.0107895.

[112] P. Jevtić, L.J. Edens, X. Li, T. Nguyen, P. Chen, D.L. Levy, Concentration-dependent Effects of Nuclear Lamins on Nuclear Size in Xenopus and Mammalian Cells., J. Biol. Chem. 290 (2015) 27557–71. doi:10.1074/jbc.M115.673798.

[113] D.-H. Kim, B. Li, F. Si, J.M. Phillip, D. Wirtz, S.X. Sun, Volume regulation and shape bifurcation in the cell nucleus., J. Cell Sci. 128 (2015) 3375–85. doi:10.1242/jcs.166330.

[114] M.B. Chen, J.A. Whisler, J. Fröse, C. Yu, Y. Shin, R.D. Kamm, On-chip human microvasculature assay for visualization and quantification of tumor cell extravasation dynamics, Nat. Protoc. 12 (2017) 865–880. doi:10.1038/nprot.2017.018.

[115] N. Saeidi, K.P. Karmelek, J.A. Paten, R. Zareian, E. DiMasi, J.W. Ruberti, Molecular crowding of collagen: A pathway to produce highly-organized collagenous structures, Biomaterials. 33 (2012) 7366–7374. doi:10.1016/J.BIOMATERIALS.2012.06.041.

[116] V. Magno, J. Friedrichs, H.M. Weber, M.C. Prewitz, M. V. Tsurkan, C. Werner, Macromolecular crowding for tailoring tissue-derived fibrillated matrices, Acta Biomater. 55 (2017) 109–119. doi:10.1016/j.actbio.2017.04.018.

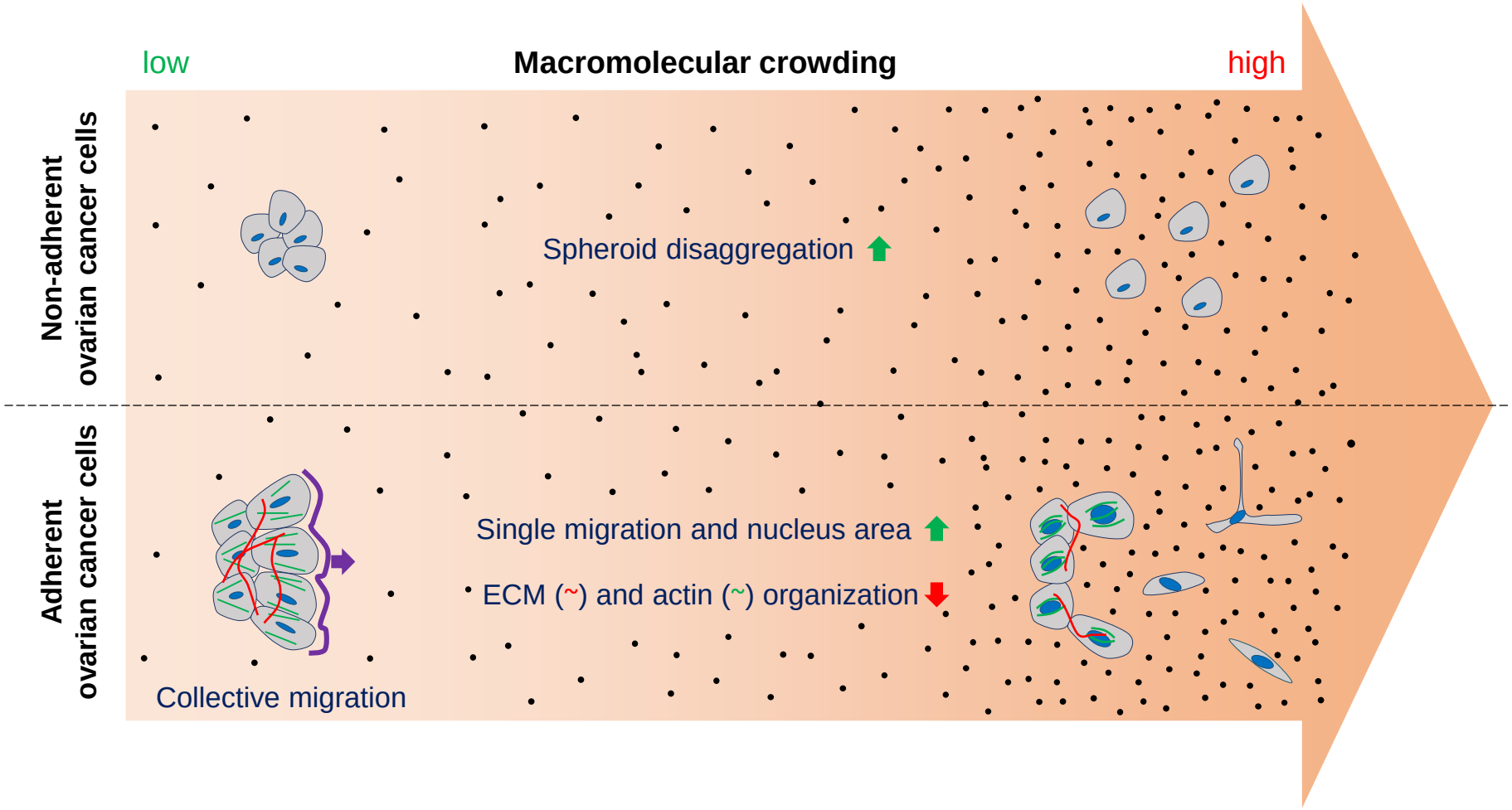
low
Macromolecular crowding
high
Non-adherent ovarian cancer cells
Spheroid disaggregation
Adherent ovarian cancer cells
Single migration and nucleus area
ECM (~) and actin (~) organization
Collective migration